Electronic Supplementary Information for

Suppressing π–π Stacking Interactions for Enhanced Solid-State Emission of Flat Aromatic Molecules via Edge Functionalization with Picket-Fence-Type Groups

Hye Jin Cho[a,‡], Sang Won Kim[b,‡], Sungjin Kim[c], Sangback Lee[d], Juhyen Lee[a], Yeonchoo Cho[b], Yunmi Lee[d], Tae-Woo Lee[c,e,f], Hyeon-Jin Shin[b], and Changsik Song*[,a]

[a] *Department of Chemistry, Sungkyunkwan University, 2066 Seobu-ro, Jangan-gu, Suwon-si, Gyeonggi-do, 16419, Republic of Korea.*

[b] *Inorganic Material Lab, Samsung Advanced Institute of Technology (SAIT), Samsung Electronics Co., Suwon 16678, Republic of Korea.*

[c] *Department of Materials Science and Engineering, Seoul National University, Seoul 08826, Republic of Korea.*

[d] *Department of Chemistry, Kwangwoon University, 20 Kwangwoon-ro, Nowon-gu, Seoul, 01897, Republic of Korea.*

[e] *School of Chemical and Biological Engineering, Seoul National University, Seoul 08826, Republic of Korea*

[f] *Institute of Engineering Research, Research Institute of Advanced Materials, Nano Systems Institute (NSI), Seoul National University, Seoul 08826, Republic of Korea*

E-mail: songcs@skku.edu

Table of Contents

1. Evaluation of the solubility and Hansen solubility parameters

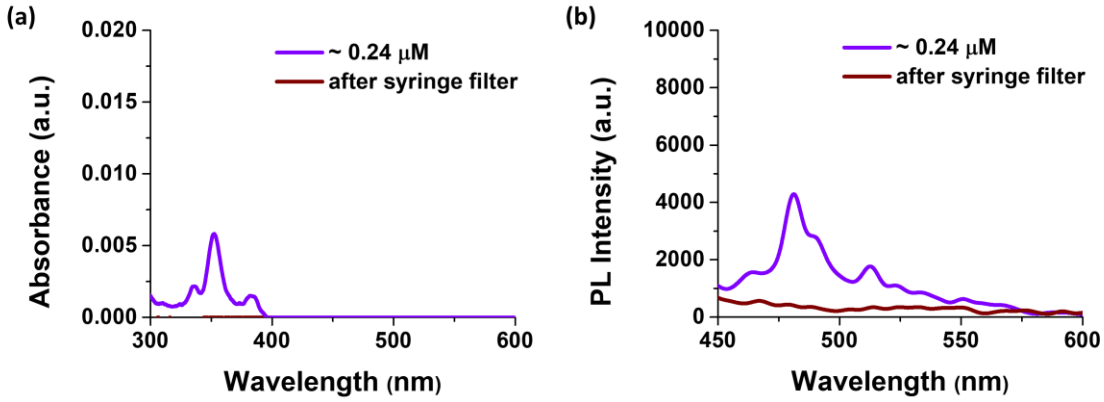

Figure S1. Absorption and emission spectra of HBC, (a) before and (b) after passing through the syringe filter.

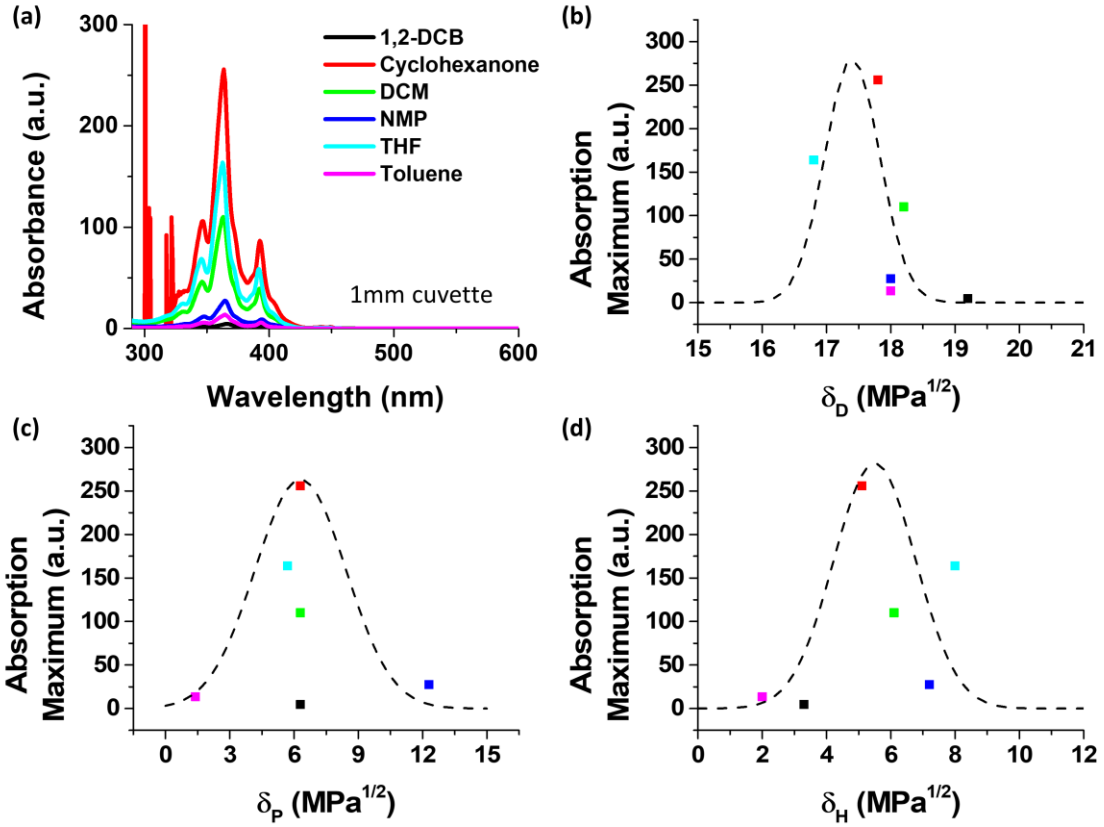

Figure S2. Absorption spectra of saturated solutions of **HBC-PF6** and Hansen solubility parameters. (a) Absorption spectra of **HBC-PF6** in 1,2-DCB, cyclohexanone, DCM, NMP, THF, and toluene. Absorption maxima from (a) for each solutions plotted as a function of

Hansen solubility parameters, (b) δ_D, (c) δ_P, and (d) δ_H (black: 1,2-DCB, red: cyclohexanone, light green: DCM, blue: NMP, cyan: THF, magenta: toluene).

Note:

Solutions (500 μL each) of six different solvents, namely 1,2-DCB, cyclohexanone, DCM, NMP, THF, and toluene, saturated with **HBC-PF6** were prepared and sonicated for 3 h at room temperature (22–25 °C) according to a previously reported method.[1] Samples were allowed to settle overnight and then centrifuged in 1.5 mL conical tubes at a speed of 13,000 rpm for 15 min, while the temperature was maintained at 20 °C. After centrifugation, the supernatants of the solutions were filtered through a syringe filter with a pore size of 200 μm and collected in 1.0 mL vials. For recording the absorption spectra, the saturated samples were diluted about 100–200-fold. The absorption spectra of the diluted samples were recorded using a quartz cell of 1 mm path length. To determine the solubility of **HBC-PF6** in wt%, the remaining saturated supernatants were dried to measure the weight of the dissolved material.

The data points in Fig. 1c are scattered and the gaussian curve does not fit well with the data points. It seemed the Hildebrand theory inherently possesses the imperfection in it; therefore, Hansen solubility parameter was introduced (Fig. S2b-d). Hansen solubility parameters are composed of three parameters of δ_D, δ_P, and δ_H. The subscript D, P, and H represents the dispersive, polar and hydrogen bonding components of intermolecular interactions, respectively. Among the three parameters, Fig. S2b gave the best fitting result. In our perspective, the dispersive force of solvents seemed to have pivotal effect on solubilizing **HBC-PF6** because it belongs to the hydrocarbon.

2. Crystallographic data for HBC-PF6

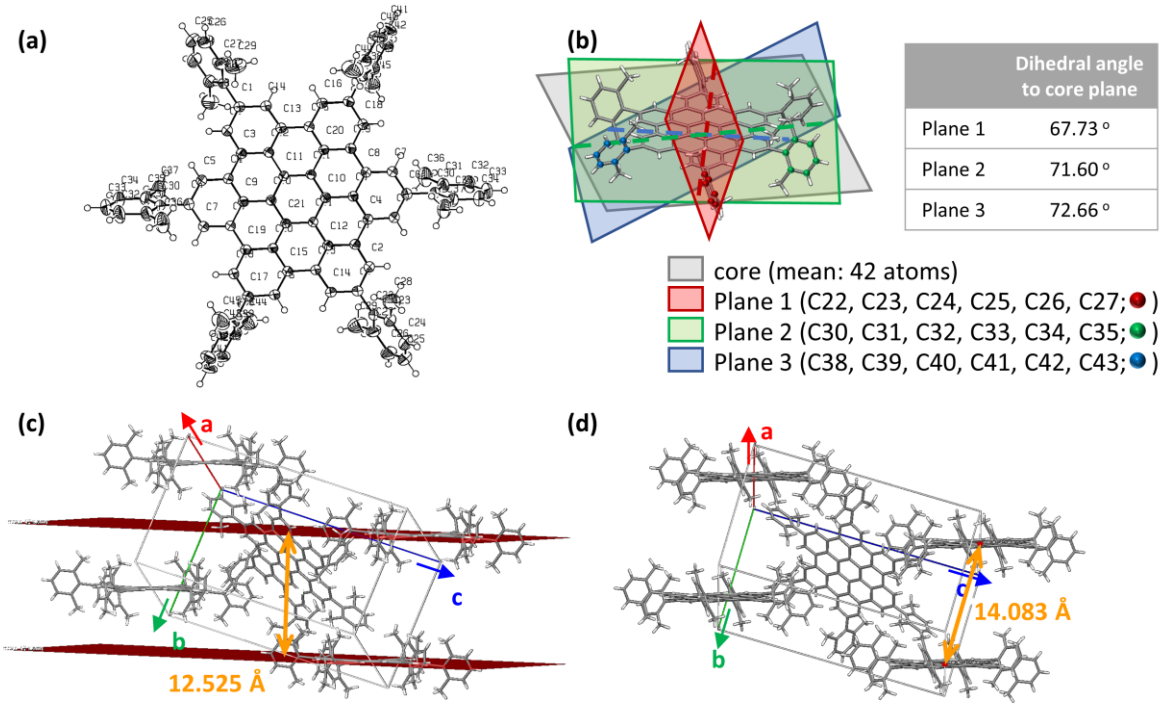

Figure S3. Single crystal structure of **HBC-PF6**. (a) Single molecular structure of **HBC-PF6**. (b) Planes and dihedral angles calculated from the structure of **HBC-PF6**. (c) The distance between two HBC core planes. (d) The distance between two HBC core centroids.

Table S1. Crystal data and structure refinement for **HBC-PF6**.

CCDC deposition number	2016559	
Empirical formula	C_{90} H_{66} (+solvent)	
Formula weight	1147.42	
Temperature	223(2) K	
Crystal system	Monoclinic	
Space group	$P2_1/c$	
Unit cell dimensions	a = 13.6749(6) Å b = 14.0833(7) Å c = 23.5926(11) Å	α = 90° β = 97.1740(10)° γ = 90°
Volume	4508.1(4) $Å^3$	
Z	2	
Density (calculated)	0.845 Mg/m^3	
Goodness-of-fit on F^2	1.047	
Final *R* indices [I>2sigma(I)]	R_1 = 0.0872, wR_2 = 0.2749	
R indices (all data)	R_1 = 0.1737, wR_2 = 0.3438	

3. Theoretical calculation

3.1. Rotational barrier

The rotational barriers were calculated as described above. Before performing a potential–energy surface scan, the structure was first optimized using the B3LYP method with the 6-31G* basis set. The scans were obtained by minimizing the potential energy under all geometrical parameters, which was achieved by varying the dihedral angle between the core and PF group in 1° increments over the 0°–360° range.

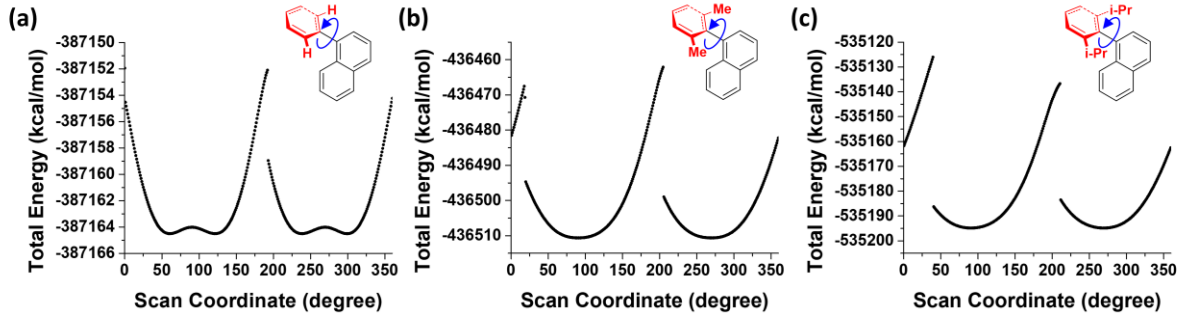

Figure S4. Rotational barrier of different PF groups on naphthalene backbone. PF groups are (a) phenyl, (b) 2,6-dimethylphenyl, and (c) 2,6-diisopropylphenyl.

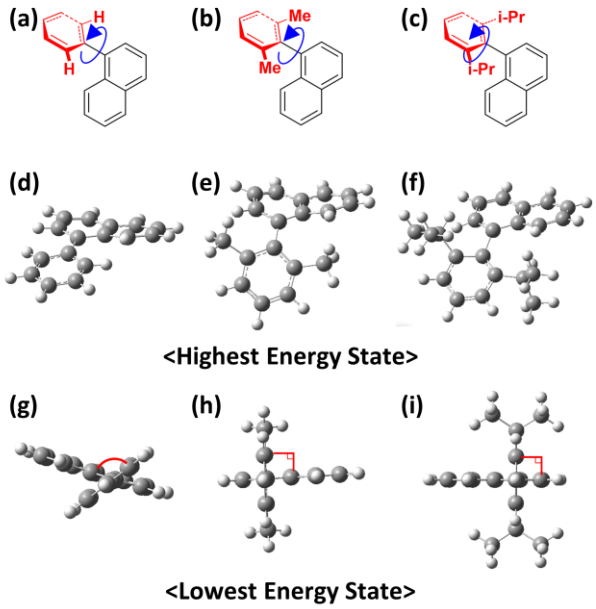

Figure S5. Structures of three different PF groups on naphthalene backbone; (a) phenyl, (b) 2,6-dimethylphenyl, and (c) 2,6-diisopropylphenyl. Corresponding structures of (a-c) in (d-f)

highest and (g-i) lowest energy states, respectively (obtained from rotational barrier calculation).

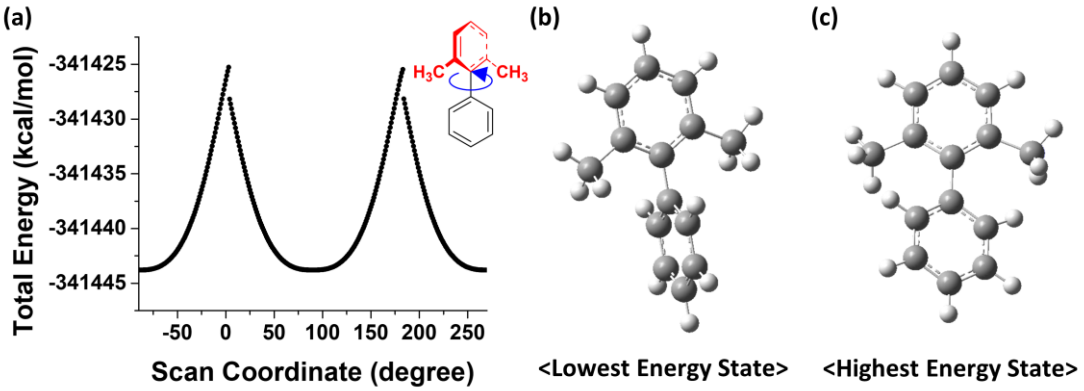

Figure S6. (a) Rotational barrier of PF group on benzene (representing the cape side of armchair periphery), with the structures in the (b) lowest and (c) highest energy states.

Note:

The edge structure of the core behaves as an important factor to optimize the PF effect. A new comparison involved a new model compound of PF group on phenyl ring (Fig. S6). For the same picket of methyl, zigzag edge from naphthalene (48.5 kcal/mol, Fig. 2c) had approximately 1.5 times higher rotational barrier than the armchair (cape side) edge from benzene (18.5 kcal/mol, Fig. S6a). The underlying reason for this difference is the existence of an additional structural parts (proton on the C8) that severely collides with PF groups when it rotates. However, the resulting energy curve and lowest energy state structure in Fig. S6 indicates that PF group still prefers to be orthogonal to the core plane, which is a prerequisite for PF effect. The equilibrium torsional angle of biphenyl structure was found to be 45.8°, with rotational barrier value of 2.0 kcal/mol.[2] PF group has approximately 10 times higher rotational barrier compared to the phenyl ring, and the equilibrium angle of 90°.

3.2. Dimer structure of pyrene

The PBE functional with D3 dispersion correction and the 6-31G* basis set were used to detect dimeric structures. The interactions governing the dimerization are dispersive attraction and Pauli repulsion, both of which are well captured at this level of computation.

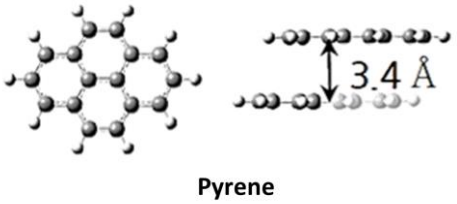

Figure S7. Structure of pyrene obtained from dimerization simulation.

3.3. HOMO-LUMO

The HOMO and LUMO energies of **Py-Ph4** and **Py-PF4** were calculated by employing TD-DFT. The TD-DFT calculations were conducted after the structure was optimized using the B3LYP method with the 6-31G* basis set.

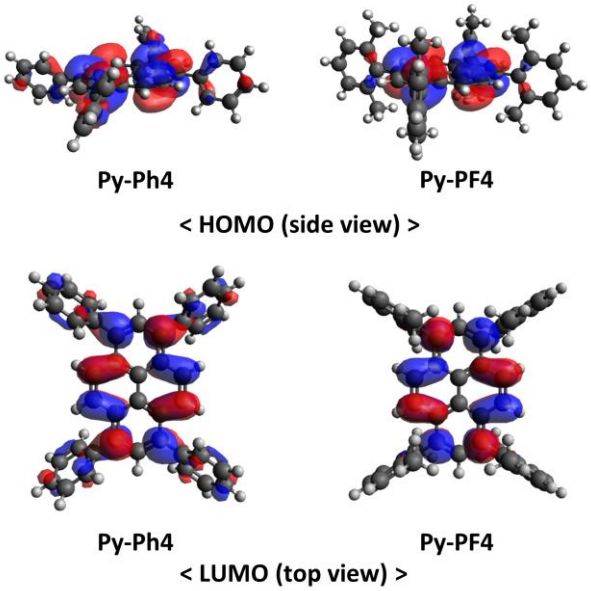

Figure S8. Optimized structure of **Py-Ph4** (left) and **Py-PF4** (right) in HOMO and LUMO states.

4. Fabrication of PAH thin films

PAH thin films were fabricated by spin-coating the stock solutions of each compound on quartz plates. The quartz plates (size: 2.5 × 3.0 cm^2) were washed with EtOH and acetone under sonication for 10 min each, and then dried under a stream of N_2. Several solutions with different concentrations were prepared by diluting the initial stock solution, and 50 μL of each sample was dropped at the center of the quartz plate, and the quartz plate was spun immediately at a speed of 3000 rpm for 60 s.

5. Evaluation of the photophysical properties

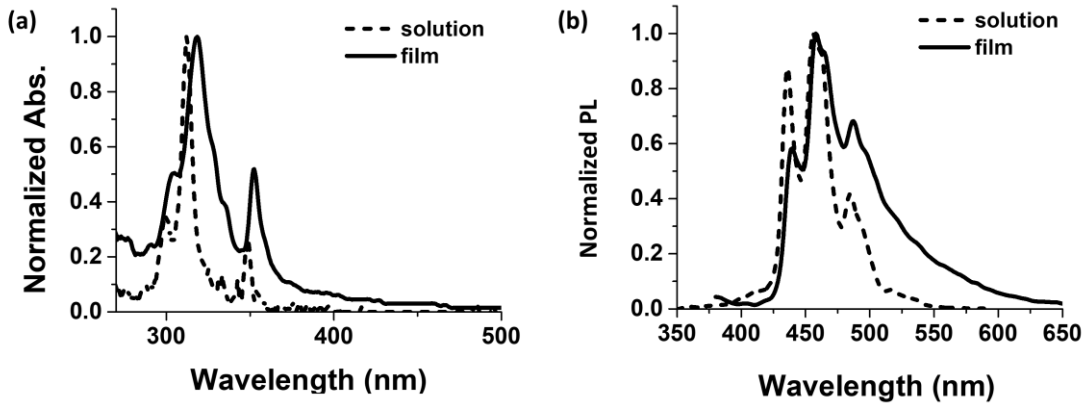

Figure S9. Absorption (a) and emission (b) spectra of **Cor-PF3**, dashed line for solution (3.0×10^{-7} M) and solid line for film (stock solution concentration of 5.0×10^{-4} M).

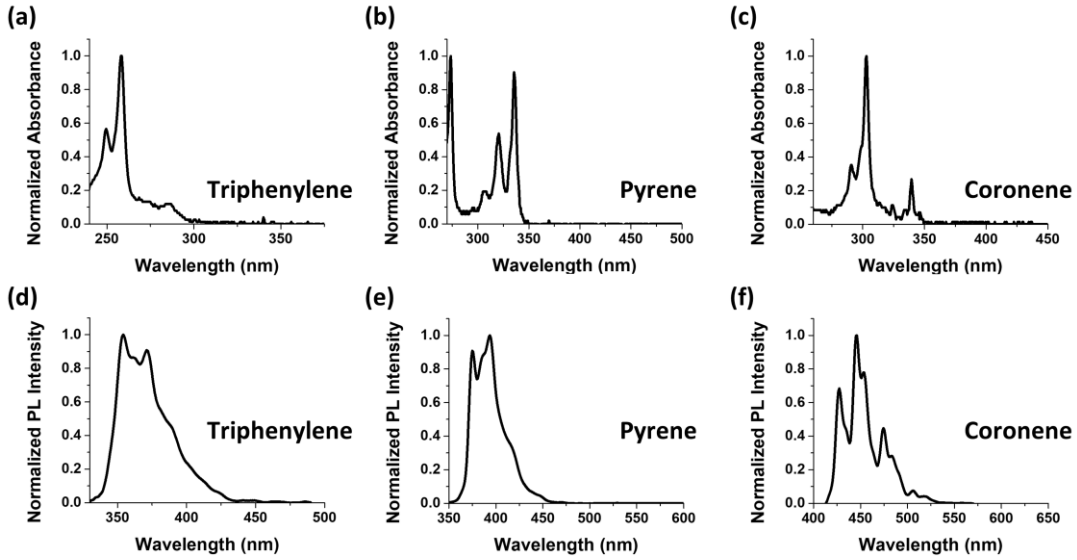

Figure S10. Absorption and Emission spectra of unsubstituted PAHs in solutions. (a,b,c) Absorption spectra of solutions. Concentrations of THF solutions: 1.0×10^{-6} M (pyrene), 3.0×10^{-7} M (triphenylene and coronene). (d,e,f) Emission spectra of solutions. Measurement conditions of 400V lamp voltage, 5 nm slit width were applied.

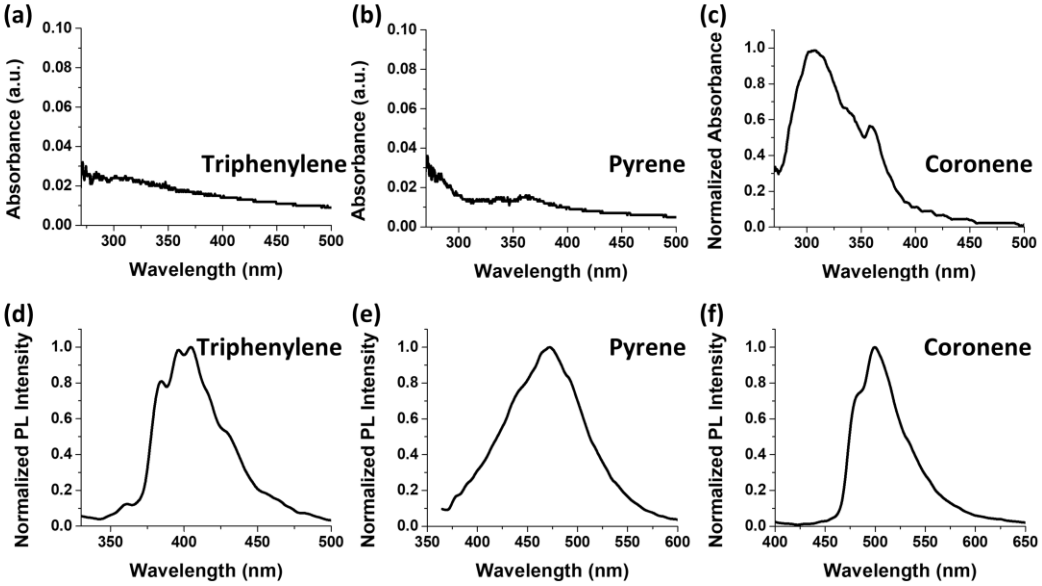

Figure S11. Absorption and emission spectra of unsubstituted PAHs in films. (a,b,c) Absorption spectra of films. Concentrations of stock solutions for thin films: 1.0×10^{-3} M (pyrene and triphenylene), 5.0×10^{-4} M (coronene). (d,e,f) Emission spectra of films. Measurement conditions of 400V lamp voltage, 5 nm slit width were applied.

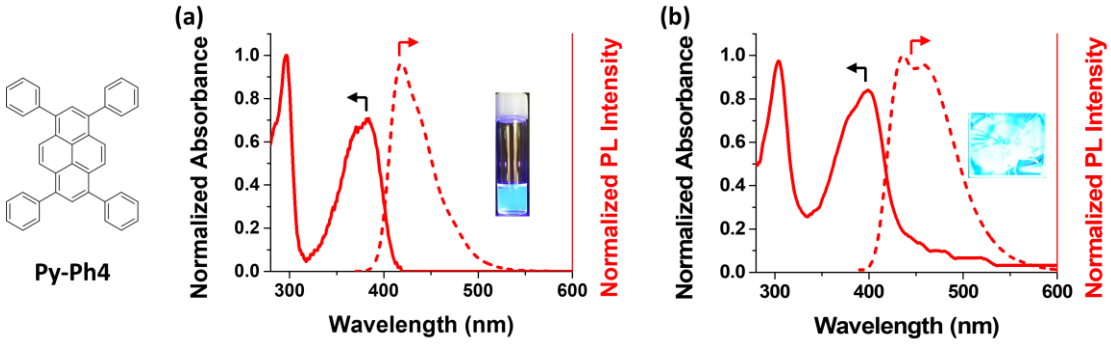

Figure S12. Absorption and emission spectra of **Py-Ph4**, (a) in THF solution (1.0×10^{-6} M) and (b) in solid-state (stock solution concentration of 5.0×10^{-4} M). Inset: **Py-Ph4** in THF solution (1.0×10^{-3} M) and film (stock solution concentration of 1.0×10^{-3} M).

6. Quantum yield (QY) measurement

The QY was calculated from linear graphs of the integrated PL intensity versus absorbance using the following equation:[3, 4]

$$\Phi_s = \Phi_i \left(\frac{\mathrm{Grad}_s}{\mathrm{Grad}_i}\right)\left(\frac{\eta_s^2}{\eta_i^2}\right)$$

where the subscripts i and s denote the standard and test samples, respectively, Φ is the fluorescence QY, Grad represents the gradient of the slope, and η is the refractive index of the solvent.

The PAHs were excited at different wavelengths: 260 nm for triphenylene; 275 nm for **TP-Ph3**; 330 nm for **Py-PF4**; 340 nm for pyrene and coronene; 350 nm for **Cor-PF3**; 360 nm for **Py-Ph4** (commonly known as 1,3,6,8-tetraphenylpyrene), **Cor-PF6**, and **HBC-PF6**; and 430 nm for **sNAP-PF8**.

Various standard materials were used for calculating the relative QY for PAHs: naphthalene for triphenylene and **TP-Ph3**; 9,10-diphenylanthracene for pyrene, **Py-Ph4**, **Py-PF4**, coronene, **Cor-PF3**, and **Cor-PF6**; quinine sulfate for **HBC-PF6**; and coumarin 153 for **sNAP-PF8**.

PL QY of the solid film samples were measured using a Quantaurus-QY absolute PL quantum yield spectrometer (C11347-11, Hamamatsu).

Note:

Contrary to our expectation, the resulting QY of **Py-Ph4** (95.2%) far exceeded that of **Py-PF4** (21.6%) in solution, because the modulated molecular orbital levels allowed $S_0 \rightarrow S_1$ transition.[5] The unexpected high QY (69.9%) observed in **TP-Ph3** could be explained in the same manner.

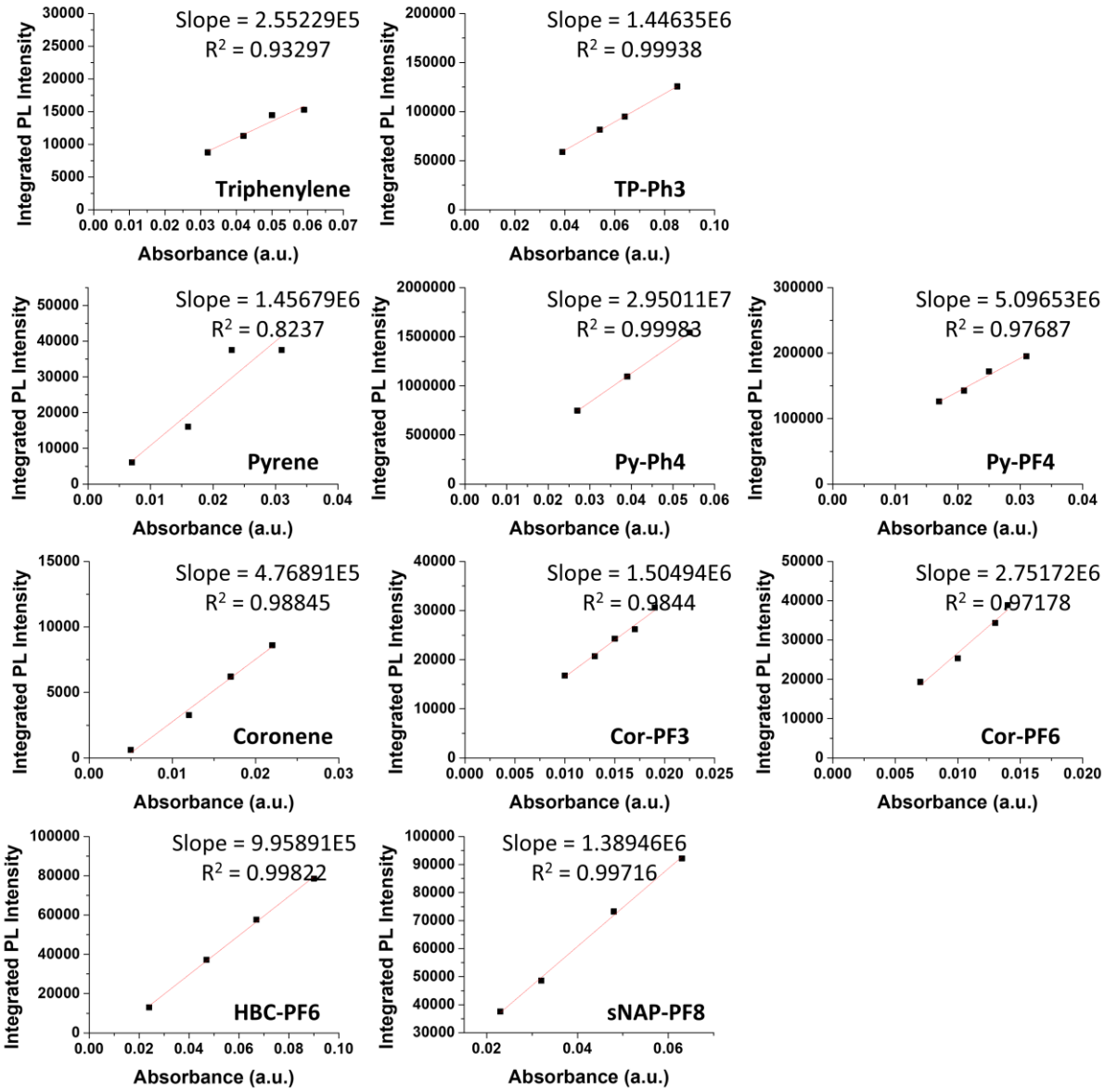

Figure S13. Integrated PL intensity to absorbance plots in solution. (PMT voltage: 400 V)

7. Time-resolved photoluminescence (TRPL) measurement

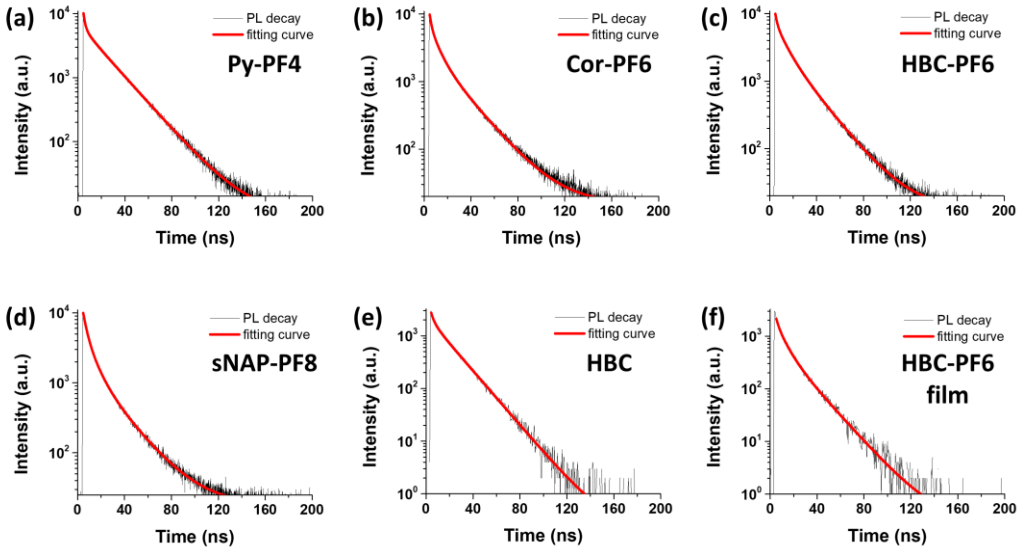

Figure S14. Time-resolved photoluminescence of the PAHs dissolved in THF. (excitation wavelength: 350 nm for solutions of **Py-PF4**, **Cor-PF6**, **HBC-PF6**, and **sNAP-PF8**; 405 nm for HBC solution and **HBC-PF6** film. Fitting curve: tri-exponential function.)

Table S2. Average lifetime (τ_{avg}), radiative (k_r) and non-radiative (k_{nr}) decay rates of PAHs.

Derivative	τ_{avg} (ns)	k_r (ns^{-1})	k_{nr} (ns^{-1})
Pyrene[a]	342	2.31×10^{3}	0.61×10^{3}
Py-PF4	2.32	9.33×10^{-2}	3.39×10^{-1}
Coronene[b]	253	-	-
Cor-PF6	3.01	2.96×10^{-2}	3.03×10^{-1}
HBC	12.0	7.53×10^{-4}	8.29×10^{-2}
HBC-PF6 (soln.)	3.64	8.52×10^{-3}	2.66×10^{-1}
HBC-PF6 (film)	9.25	5.84×10^{-3}	1.02×10^{-1}
sNAP-PF8	8.75	5.37×10^{-3}	1.09×10^{-1}

[a] In THF, ref[6]. [b] In 1,2,4-trichlorobenzene (TCB), ref[7].

Note:

Samples for TRPL measurement were prepared as follows: PF-functionalized PAHs were dissolved in THF at a few tenths of μM. HBC (1 mg) was dispersed in THF (4 mL) by sonicating for 1 h in ambient condition, and the supernatant of the solution was employed. The

100 μM stock solution of **HBC-PF6** in THF was spin-coated on quartz plate (2.5 × 2.5 cm^2) to make film.

While the HBC film was non-emissive, the film of HBC-PF6 exhibited similar decay curve to that of solution, which coincide with our statement on PF effect.

8. Comparison of the parameters in luminous elements of HBC-PF6 and other nanographene-based emitters

Table S3. OLED parameters reported in previous literatures and this work.

PAH emitter (# of aromatic rings)	EL color	FWHM /nm	EQE /%	CE[a] /cd A^{-1}	L_{max}[b] /cd m^{-2}	V_T[c] /V	Device	Ref.
Diboradibenzo-chrysene (6)	Green	62	2.9	15.8	-	2.6	OLED	[8]
Hexabenzo-ovalene (16)	Red	>100	0.78	-	242	-	LEC	[9]
Hexabenzoborazinocoronene (13)	White	>100	-	3	50	-	LEC	[10]
HBC-aggregate (13)	Green	72	0.5	-	-	-	OLED	[11]
Dibenzo-naphtho-pentacene (9)	Blue-green	92	0.4	-	-	-	OLED	[11]
Dibenzo-phenanthro-pentaphene (10)	Green	100	0.3	-	-	-	OLED	[11]
HBC-PF6 (13)	Blue	20	1.23	2.59	1243	3.8	OLED	This work

[a] Current efficiency. [b] Maximum luminance. [c] Turn-on voltage.

9. Preparation of PF-functionalized PAHs

9.1. Synthesis detail

Most of the solvents used in the experiments were purchased from Samchun Pure Chemical, including tetrahydrofuran (THF, 99.9%), ethyl acetate (EA, 99.5%), hexane (95%), dichloromethane (DCM, 99.5%), ethanol (95%), methanol (99.5%), chloroform (99.5%), 1,4-dioxane (99.5%), diphenyl ether (99.5%), and nitromethane (99%). Among them, EA, DCM, hexane, ethanol, methanol, and chloroform were used without further purification. Spectrophotometric grade solvents including 1,2-dichlorobenzene (1,2-DCB), dichloromethane (DCM), N-methyl-2-pyrrolidone (NMP) were obtained from Alfa Aesar, while toluene was obtained from Tokyo Chemical Industry Co., Ltd. Cyclohexanone (99.5%) was purchased from Samchun Pure Chemical.

Potassium carbonate (99.5%), hydrochloric acid (35.0~37.0%), triethylamine (99%), and sodium thiosulfate (98%) were also purchased from Samchun Pure Chemical. N-butyl lithium (2.5M in hexane), trimethyl borate (98%), phenylboronic acid (95%), tetrakis(triphenylphosphine)palladium(0) (99%), [1,1′-bis(diphenylphosphino)ferrocene]dichloropalladium(II) (complex with dichloromethane), copper iodide (98%), iron powder (99%), platinum(II) chloride (98%), and iron(III) chloride (97%) were purchased from Sigma-Aldrich. 2-Bromo-1,3-dimethylbenzene (98%), 1,3,6,8-tetrabromopyrene (98%), and coronene (83%) were ob-tained from Tokyo Chemical Industry Co., Ltd. Cesium carbonate (99%) was obtained from Alfa Aesar. Bromine (99%) and nitrobenzene (99%) were purchased from Jun-sei Chemical Co., Ltd.

■ **Experimental procedure for synthesis of 2,6-dimethylphenylboronic acid (PF-B(OH)$_2$)**

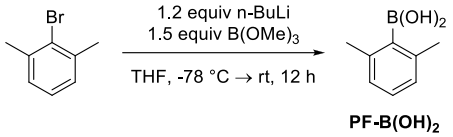

2,6-dimethylphenylboronic acid (PF-B(OH)$_2$). Prepared with modified procedure of previous literatures.[12, 13] A flame-dried 100 mL round-bottomed flask equipped with a stirring bar was charged N_2. Dry THF (32 mL) and 2-bromo-1,3-dimethylbenzene (2.2 mL, 16.2 mmol) were added via syringe, stirred, followed by cooling to -78 ℃ in a dry ice-acetone bath. N-butyl lithium (2.5 M solution in hexane, 7.8 mL, 19.5 mmol) was added dropwise via syringe, and the mixture was stirred at -78 ℃ for 1 h. Trimethyl borate (5 mL, 24.3 mmol) was then added dropwise via syringe. The turbid reaction mixture was then changed into clear solution, allowed to warm to room temperature. After stirring for additional 6 h, it became turbid again and quenched with 2 M aqueous HCl (20 mL). The reaction mixture was extracted with ethyl acetate (3 × 30 mL) and the combined extract was washed with brine (100 mL), dried over anhydrous Na_2SO_4 and concentrated *in vacuo*. The resulting oil was then suspended in hexane (100 mL), giving recrystallized **PF-B(OH)$_2$** as white solid. The resulting solid was collected by filtration and washed with hexane to afford the desired product (1.19 g, 49% yield). **IR** (neat): ; **^{1}H NMR** (500 MHz, $CDCl_3$): δ 7.16 (t, J = 7.6 Hz, 1H), 6.99 (d, J = 7.6 Hz, 2H), 4.63 (s, 2H), 2.38 (s, 6H); **^{13}C NMR** (125 MHz, $CDCl_3$): δ 139.5, 128.9, 126.4. 22.2; **HRMS** (EI) calcd. for $C_8H_{11}BO_2$: *m/z* 150.0852 ([M]$^+$), found: *m/z* 150.0856 ([M]$^+$).

■ **Experimental procedure for synthesis of 1,5,9-triphenyltriphenylene (TP-Ph3)**

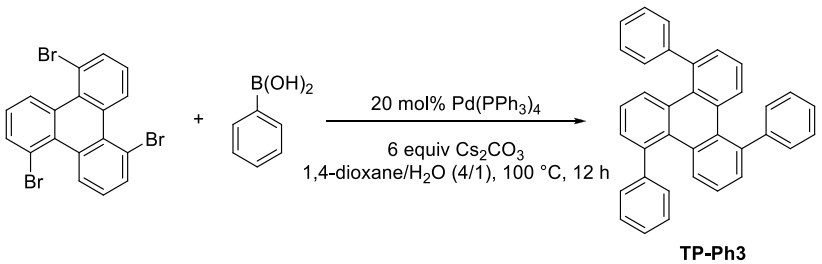

1,5,9-Triphenyltriphenylene (TP-Ph3). 1,5,9-Tribromotriphenylene[14] (10.0 mg, 0.0215 mmol), phenylboronic acid (15.7 mg, 0.129 mmol), $Pd(PPh_3)_4$ (5.0 mg, 0.00430 mmol) and Cs_2CO_3 (42.0 mg, 0.129 mmol) were added to a vial (8 mL) charged with a magnetic bar in a glove box. The vial was sealed with a cap (phenolic open top cap with gray PTFE/silicon) and removed from the glove box. Then, it was purged with N_2 gas and dioxane/H_2O (1.25 mL, 4/1) was added under N_2. The reaction mixture was allowed to stir at 100 °C for 12 h. After that time, the reaction solution was quenched by adding water (1 mL), and the mixture was washed with CH_2Cl_2 (3 × 1 mL). The combined organic layers were dried over $MgSO_4$, filtered and concentrated. The crude product was purified using silica gel column chromatography (100%

hexanes 100%), affording the desired product **TP-Ph3** (5.80 mg, 59%) as a white solid. **^{1}H NMR** (400 MHz, $CDCl_3$): δ 7.63 (dd, *J* = 8.2, 1.3 Hz, 3H), 7.45-7.35 (m, 15H), 7.31 (dd, *J* = 7.3, 1.3 Hz, 3H), 7.04 (dd, *J* = 8.2, 7.4 Hz, 3H); **^{13}C NMR** (100 MHz, $CDCl_3$): δ 145.2, 139.8, 131.4, 130.8, 130.0, 129.3, 128.8, 128.6, 126.8, 124.4; **HRMS** (ESI) calcd. for $C_{36}H_{24}$: *m/z* 456.1878 ($[M]^+$), found: *m/z* 456.1878 ($[M]^+$).

■ Experimental procedure for synthesis of 1,3,6,8-tetrakis(2,6-dimethylphenyl)pyrene (Py-PF4)

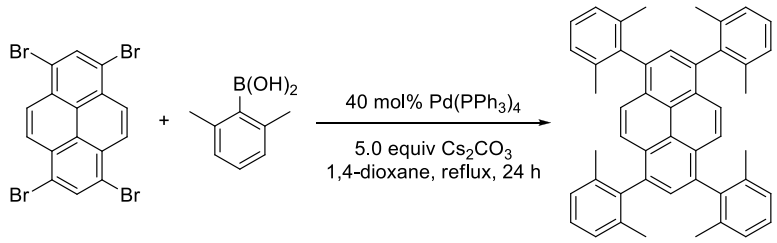

Py-PF4

1,3,6,8-Tetrakis(2,6-dimethylphenyl)pyrene (Py-PF4). 1,3,6,8-Tetrabromopyrene (100 mg, 0.189 mmol), **PF-B(OH)$_2$** (142 mg, 0.946 mmol), $Pd(PPh_3)_4$ (88.0 mg, 0.0757 mmol), and Cs_2CO_3 (312 mg, 0.946 mmol) were added to a 25 ml pressure tube with a magnetic bar inside. After placed under the vacuum for 5 minutes and recharged with N_2, 2.1 mL of 1,4-dioxane was added. The pressure tube was sealed with a PTFE cap, both front and back sealed with FETFE O-ring. The reaction mixture was allowed to stir, refluxed for 24 h. The resultant mixture was then cooled to the room temperature, quenched by adding water (5 mL). The mixture was extracted with CH_2Cl_2 (3 × 5 mL). The combined organic layers were dried over anhydrous Na_2SO_4 and concentrated *in vacuo*. The crude product was purified by column chromatography on silica gel (using CH_2Cl_2/hexane = 1/9 as eluent) to afford desired product **Py-PF4** (57.3 mg, 49% yield) as pale yellow solid. **^{1}H NMR** (500 MHz, $CDCl_3$): δ 7.63 (s, 2H), 7.53 (s, 4H), 7.25 (dd, *J* = 8.2, 6.6 Hz, 4H), 7.18 (d, *J* = 7.5 Hz, 8H), 1.99 (s, 24H); **^{13}C NMR** (125 MHz, $CDCl_3$): δ 140.0, 136.9, 136.3, 128.5, 128.3, 127.4, 127.3, 125.9, 124.8, 20.8; **HRMS** (EI) calcd. for $C_{48}H_{42}$: *m/z* 618.3287 ($[M]^+$), found: *m/z* 618.3263 ($[M]^+$).

■ **Experimental procedure for synthesis of 1,5,9-tris(2,6-dimethylphenyl)coronene (Cor-PF3)**

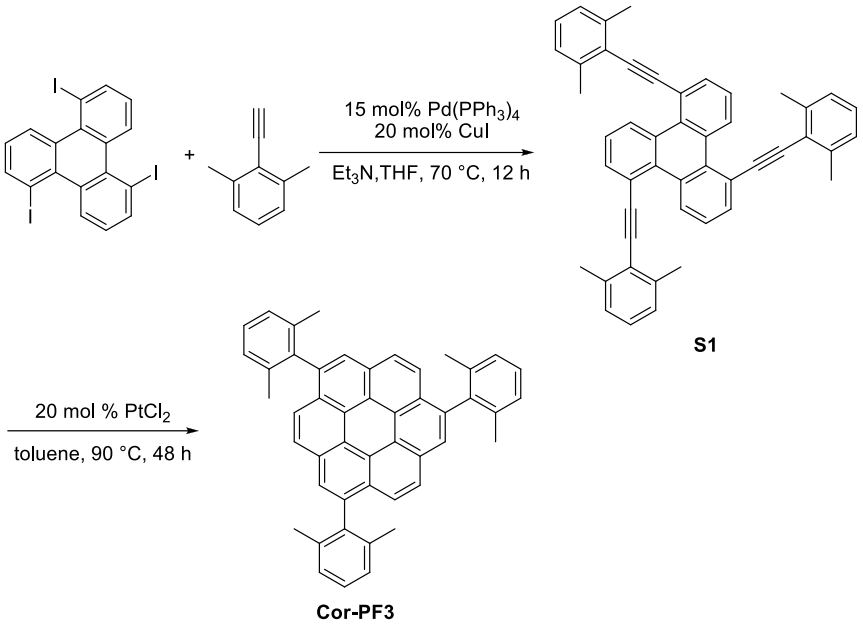

1,5,9-Tris((2,6-dimethylphenyl)ethynyl)triphenylene (S1). 1,5,9-Triiodotriphenylene[15] (3.20 mg, 5.28 x 10^{-3} mmol), CuI (0.200 mg, 1.06 x 10^{-3} mmol) and $Pd(PPh_3)_4$ (0.900 mg, 7.92 x 10^{-4} mmol) were adaded to a vial (8 mL) charged with a magnetic bar in a glove box. The vial was sealed with a cap (phenolic open top cap with gray PTFE/silicon) and removed from the glove box. After the vial was purged with N_2 gas, THF (0.8 mL), Et_3N (0.5 mL) and 2-ethynyl-1,3-dimethylbenzene (2.50 mg, 0.0190 mmol) were added to vial sequentially. Then, the reaction mixture was stirred at 70 °C for 12 h. After that time, the reaction solution was quenched by adding water (1 mL) and washed with CH_2Cl_2 (3 × 1 mL). The combined organic layers were dried over $MgSO_4$, filtered and concentrated. The crude product was purified using silica gel column chromatography (100% hexanes), affording the desired product **S1** (2.80 mg, 86.5%) as a white solid. **^{1}H NMR** (400 MHz, $CDCl_3$): δ 10.06 (dd, *J* = 8.3, 1.2 Hz, 3H), 7.99 (dd, *J* = 7.4, 1.2 Hz, 3H), 7.55 (t, *J* = 8.0, 3H), 7.21-7.17 (m, 3H), 7.14-7.12 (m, 6H), 2.63 (s, 18H); **^{13}C NMR** (100 MHz, $CDCl_3$): δ 140.6, 135.7, 131.1, 130.7, 128.0, 127.6, 126.9, 125.4, 123.3, 119.8, 100.1, 93.0, 21.4; **HRMS** (ESI) calcd. for $C_{48}H_{36}$: *m/z* 612.2817 ($[M]^+$), found: *m/z* 612.2816 ($[M]^+$).

1,5,9-Tris(2,6-dimethylphenyl)coronene (Cor-PF3). S1 (16.0 mg, 0.0261 mmol) and $PtCl_2$ (1.40 mg, 0.00522 mmol) were added to a vial (8 mL) charged with a magnetic bar in a glove box. The vial was sealed with a cap (phenolic open top cap with gray PTFE/silicon) and removed from the glove box. Then, it was purged with N_2 gas and toluene (0.26 mL) was added to vial under N_2. The reaction mixture was stirred at 90 °C for 48 h. After that time, the reaction solution was concentrated under vacuo. The crude product was purified using silica gel column

chromatography (100% hexanes, affording the desired product **Cor-PF3** (9.70 mg, 61%) as a white solid. **^{1}H NMR** (400 MHz, $CDCl_3$): δ 8.82 (d, *J* = 8.7 Hz, 3H), 8.74 (s, 3H), 8.47 (d, *J* = 8.7 Hz, 3H), 7.47-7.44 (m, 3H), 7.38 (d, *J* = 7.5 Hz, 6H), 2.04 (s, 18H); **^{13}C NMR** (100 MHz, $CDCl_3$): δ 140.2, 137.7, 137.5, 128.8, 127.7, 127.6, 127.4, 126.4, 124.1, 122.3, 20.7; **HRMS** (ESI) calcd. for $C_{48}H_{36}$: *m/z* 612.2817 ($[M]^+$), found: *m/z* 612.2817 ($[M]^+$).

■ Experimental procedure for synthesis of 1,4,5,8,9,12-Hexakis(2,6-dimethylphenyl)coronene (Cor-PF6)

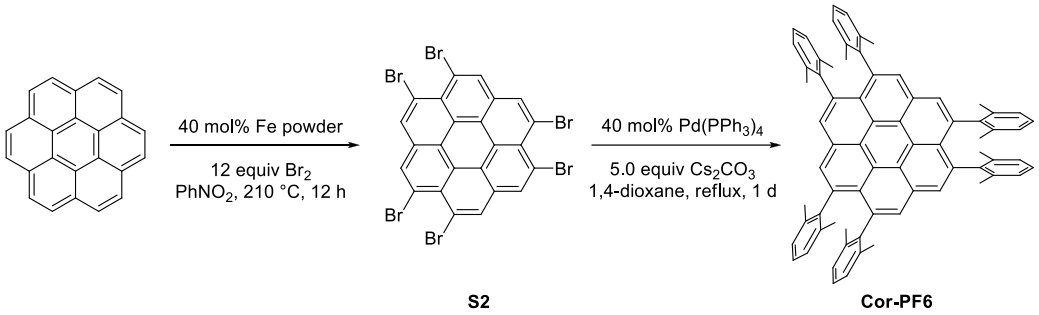

S2 Cor-PF6

1,4,5,8,9,12-Hexabromocoronene (S2). Coronene (500 mg, 1.38 mmol) and iron powder (31.0 mg, 0.553 mmol) were added to a 25 mL two-neck round-bottomed flask equipped with a magnetic stirring bar and a reflux condenser. Afterwards 14 mL nitrobenzene was added and the coronene was soon dissolved clearly. To a stirred solution, 0.845 mL of bromine was added dropwise under room temperature, forming precipitate immediately. The reaction mixture was allowed to refluxed for 12 h at 210 ℃. The resultant mixture was cooled to the room temperature, quenched with 10 mL of saturated aqueous sodium thiosulfate. 10 mL $CHCl_3$ was added to dilute the mixture and the organic phase with precipitate was collected. The precipitated solid was collected by filtration. The given solid was dispersed in 30 mL $CHCl_3$, sonicated for 20 min, recollected after washing with $CHCl_3$ and MeOH. Again, the solid was dispersed in 30 mL MeOH by sonicating for 20 min, recollected by washing thoroughly with $CHCl_3$ and MeOH until the deep dark violet color of filtrate fades. The obtained solid (1.05 g) was used for the next reaction without further purification.

1,4,5,8,9,12-Hexakis(2,6-dimethylphenyl)coronene (Cor-PF6). S2 (270 mg, 0.349 mmol assuming that the solid is pure), **PF-B(OH)2** (420 mg, 2.79 mmol), $Pd(PPh_3)_4$ (163 mg, 0.140 mmol), and Cs_2CO_3 (919 mg, 2.79 mmol) were added to a 25 ml pressure tube with a magnetic bar inside. After placed under the vacuum for 5 minutes and recharged with N_2, 3.5 mL of 1,4-dioxane was added. The pressure tube was sealed with a PTFE cap, both front and back sealed with FETFE O-ring. The reaction mixture was allowed to stir, refluxed for 24 h. The resultant mixture was then cooled to the room temperature, quenched by adding water (5 mL). The mixture was extracted with CH_2Cl_2 (3 × 5 mL). The combined organic layers were dried over anhydrous Na_2SO_4 and concentrated *in vacuo*. The crude product was purified by preparative

thin layer chromatography on silica gel (using CH_2Cl_2/hexane = 1/9 as eluent) to afford mixture of desired product **Cor-PF6** with its regioisomers (36.2 mg, 11% yield) as yellow solid. **^{1}H NMR** (500 MHz, $CDCl_3$): δ 8.25-8.21 (m, 6H), 7.32-7.27 (m, 6H), 7.23 (d, *J* = 7.5 Hz, 9H), 7.15 (dt, *J* = 15.3, 6.5 Hz, 1H), 7.06-7.01 (m, 2H), 1.99-1.83 (singlet peaks each, total 36 H); **^{13}C NMR** (125 MHz, $CDCl_3$): δ 140.4, 137.8, 137.7, 137.2, 127.7, 127.6, 127.5, 127.4, 127.4, 124.3, 122.7, 21.4, 20.5; **HRMS** (FAB) calcd. for $C_{72}H_{60}$: *m/z* 925.4773 ($[M+H]^+$), found: *m/z* 925.4786 ($[M+H]^+$).

■ Experimental procedure for synthesis of 1,4,5,8,9,12-Hexakis(2,6-dimethylphenyl)coronene (HBC-PF6)

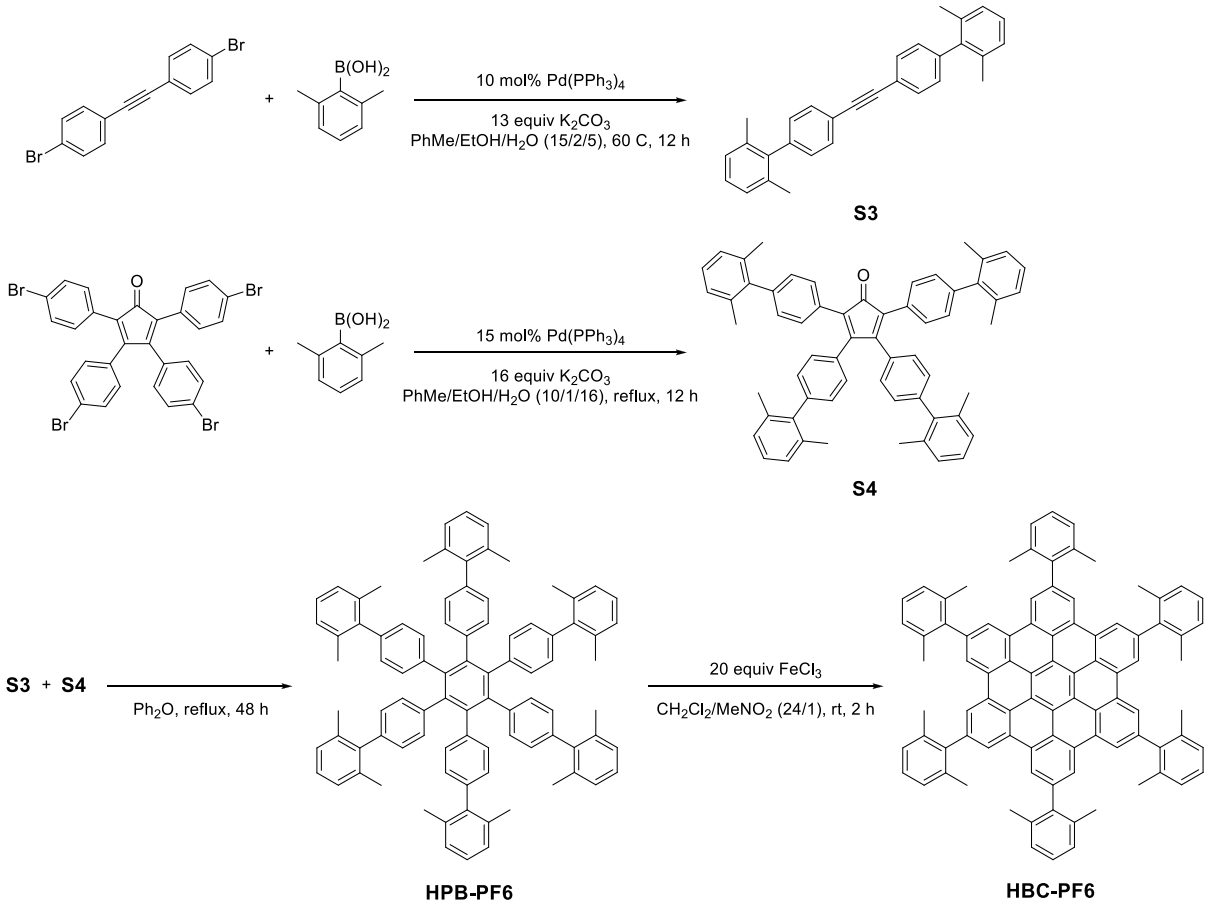

1,2-bis(2',6'-dimethylbiphenyl-4-yl)ethyne (S3). A 50 mL two-neck round-bottomed flask equipped with a magnetic stirring bar and a reflux condenser was charged with bis(4-bromophenyl)acetylene[16] (340 mg, 1.01 mmol), **PF-B(OH)$_2$** (380 mg, 2.53 mmol), and $Pd(PPh_3)_4$ (118 mg, 0.101 mmol). Afterwards 20 mL of toluene was added followed by the addition of 2.7 mL ethanol. To this solution, a degassed aqueous solution of K_2CO_3 (1.9 g in 6.7 mL DI water, 13.6 mmol) were added. The reaction mixture was allowed to stir, refluxed for 12 h. The resultant mixture was then cooled to the room temperature. The mixture was extracted with CH_2Cl_2 (3 × 20 mL). The organic layers were combined and washed with brine

(50 mL). The collected organic layer was dried over anhydrous Na_2SO_4 and concentrated *in vacuo*. The crude product was purified by column chromatography on silica gel (using CH_2Cl_2/hexane = 1/9 as eluent) to afford desired product **S3** (242 mg, 62% yield) as white solid. **^{1}H NMR** (500 MHz, $CDCl_3$): δ 7.62 (d, *J* = 8.2 Hz, 4H), 7.20-7.17 (m, 2H), 7.16 (d, *J* = 8.2 Hz, 4H), 7.12 (d, *J* = 7.6 Hz, 4H), 2.05 (s, 12H); **^{13}C NMR** (125 MHz, $CDCl_3$): δ 141.3, 141.2, 135.9, 131.8, 129.2, 127.4, 127.3, 121.6, 89.4, 20.8; **HRMS** (EI) calcd. for $C_{30}H_{26}$: *m/z* 386.2035 ($[M]^+$), found: *m/z* 386.2061 ($[M]^+$).

2,3,4,5-tetrakis(2',6'-dimethylbiphenyl-4-yl)cyclopenta-2,4-dienone (S4). 2,3,4,5-tetrakis(4-bromophenyl)cyclopenta-2,4-dienon[17] (179 mg, 0.256 mmol), **PF-B(OH)$_2$** (169 mg, 1.13 mmol), Pd(dppf)Cl_2·CH_2Cl_2 (32.6 mg, 0.0399 mmol), and Cs_2CO_3 (501 mg, 1.54 mmol) were added to a 25 ml pressure tube with a magnetic bar inside. After placed under the vacuum for 5 minutes and recharged with N_2, 6 mL toluene was added. 0.5 mL EtOH and 1 mL DI water were added right after the degassing for 30 min. The pressure tube was sealed with a PTFE cap, both front and back sealed with FETFE O-ring. The reaction mixture was allowed to stir, refluxed for 24 h. The resultant mixture was then cooled to the room temperature. The mixture was extracted with CH_2Cl_2 (3 × 20 mL). The organic layers were combined and washed with brine (50 mL). The collected organic layer was dried over anhydrous Na_2SO_4 and concentrated *in vacuo*. The crude product was purified by column chromatography on silica gel (using CH_2Cl_2/hexane = 1/2 as eluent) to afford desired product **S4** (184 mg, 90% yield) as dark purple solid. **^{1}H NMR** (500 MHz, $CDCl_3$): δ 7.43 (d, *J* = 8.3 Hz, 4H), 7.17-7.13 (m, 4H), 7.13-7.07 (m, 12H), 7.06 (d, *J* = 8.3 Hz, 4H), 7.01 (d, *J* = 8.3 Hz, 4H), 2.05 (s, 12H), 1.98 (s, 12H); **^{13}C NMR** (125 MHz, $CDCl_3$): δ 200.9, 154.9, 141.5, 141.4, 141.2, 140.3, 136.1, 135.7, 132.0, 130.1, 129.5, 129.2, 128.8, 128.7, 127.3, 127.3, 127.2, 127.1, 125.0, 20.8, 20.5; **HRMS** (FAB) calcd. for $C_{61}H_{52}O$: *m/z* 801.4096 ($[M+H]^+$), found: *m/z* 801.4090 ($[M+H]^+$).

Hexa-2,6-dimethylphenyl-hexaphenylbenzene (HPB-PF6). S3 (114 mg, 0.294 mmol) and **S4** (196 mg, 0.245 mmol) were added to a 10 mL two-neck round-bottomed flask equipped with a magnetic stirring bar and a reflux condenser. After the addition of 2.5 mL diphenyl ether, the reaction mixture was allowed to stir, refluxed vigorously for 48 h using a heating mantle. The initial dark purple color of the reaction mixture changed to red-brown, finally turned into clear orange at the end of the reaction. The resultant mixture was then cooled to the room temperature, diluted with EtOH to give orange precipitate. The precipitate was collected by filtration, recrystallized from diphenyl ether. The recrystallized solid was then collected by filtration, washed with ethanol and hexane, and dried to give desired product **HPB-PF6** (229 mg, 81% yield) as white crystalline solid. **^{1}H NMR** (500 MHz, $CDCl_3$): δ 7.11 (dd, *J* = 8.0, 7.0 Hz, 6H), 7.03 (d, *J* = 8.1 Hz, 12H), 7.03 (d, *J* = 7.4 Hz, 12H), 6.71 (d, *J* = 8.1 Hz, 12H), 1.84 (s, 36H); **^{13}C NMR** (125 MHz, $CDCl_3$): δ 141.8, 140.5, 139.4, 138.0, 136.0, 132.0, 127.3, 127.0, 126.8, 20.6; **HRMS** (FAB) calcd. for $C_{90}H_{78}$: *m/z* 1159.6182 ($[M+H]^+$), found: *m/z* 1159.6296 ($[M+H]^+$).

2,5,8,11,14,17-hexakis(2,6-dimethylphenyl)hexabenzo[*bc,ef,hi,kl,no,qr*]coronene (HBC-PF6). HPB-PF6 (200 mg, 0.172 mmol) was added in 100 mL round-bottomed flask followed by the addition of 29 mL methylene chloride. The mixture was stirred with N_2 bubbling through it and a solution of $FeCl_3$ (580 mg, 3.45 mmol) in 1.2 mL nitromethane was soon added. The reaction mixture was kept stirred under room temperature with N_2 bubbling for 2 h. The reaction was quenched by addition of 3 mL MeOH, extracted with CH_2Cl_2 (3 × 30 mL). The organic layers were combined and washed with brine (80 mL). The collected organic layer was dried over anhydrous Na_2SO_4 and concentrated *in vacuo*. The crude product was purified by column chromatography on silica gel (using CH_2Cl_2/hexane = 1/5 as eluent) to afford desired product **HBC-PF6** (118 mg, 60% yield) as yellow solid. **^{1}H NMR** (500 MHz, $CDCl_3$): δ 9.04 (s, 12H), 7.29 (dd, *J* = 8.7, 6.2 Hz, 6H), 7.25 (d, *J* = 6.6 Hz, 12H), 2.27 (s, 36H); **^{13}C NMR** (125 MHz, $CDCl_3$): δ 141.9, 140.1, 136.3, 131.1, 127.7, 127.6, 124.7, 123.3, 121.3, 21.5; **HRMS** (FAB) calcd. for $C_{90}H_{66}$: *m/z* 1147.5243 ($[M+H]^+$), found: *m/z* 1147.5228 ($[M+H]^+$).

■ Experimental procedure for synthesis of PF-functionalized supernaphthalene (sNAP-PF8)

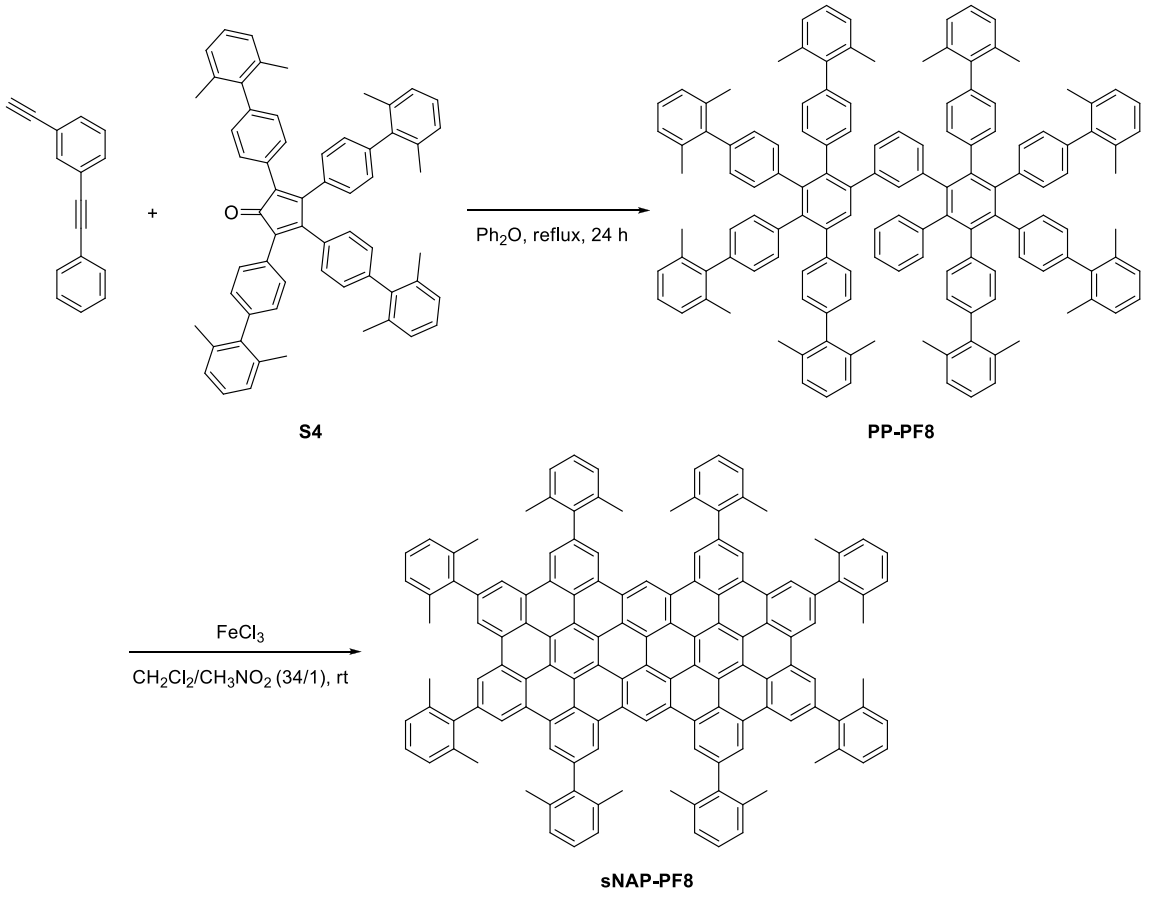

PF-functionalized polyphenylene precursor (PP-PF8). 3-ehynyldiphenylacetylene[18] (30.6 mg, 0.151 mmol), and **S4** (302.6 mg, 0.378 mmol) were added to a 10 mL two-neck round-bottomed flask equipped with a magnetic stirring bar and a reflux condenser. After the addition of 2.5 mL diphenyl ether, the reaction mixture was allowed to stir, refluxed vigorously for 49 h using a heating mantle. The resultant mixture was then cooled to the room temperature and the solvent was removed while heating it to 70 ℃ *in vacuo*. The crude is purified by preparative thin layer chromatography on silica gel (using CH_2Cl_2/hexane = 1/2 as eluent) to afford white solid which the desired product **PP-PF8** (115.3 mg) mixed with impurities; **MS** (MALDI-TOF, positive) calcd. for $C_{136}H_{114}$: *m/z* 1747.9 ($[M+H]^+$), found: *m/z* 1747.4 ($[M+H]^+$).

PF-functionalized supernaphthalene (sNAP-PF8). The mixture of **PP-PF8** (10 mg, assuming 0.006 mmol) was added in 50 mL round-bottomed flask followed by the addition of 34 mL methylene chloride. The mixture was stirred with N_2 bubbling through it and a solution of $FeCl_3$ (158 mg, 0.972 mmol) in 1 mL nitromethane was soon added. The reaction mixture was kept stirred under room temperature with N_2 bubbling for 24 h. The reaction was quenched by addition of 10 mL MeOH and concentrated *in vacuo*. The precipitates were dispersed in MeOH, centrifuged to obtain a crude solid. The crude was purified by preparative thin layer chromatography on silica gel (using CH_2Cl_2/hexane = 1/3 as eluent) to afford desired product **sNAP-PF8** (8 mg, 81% yield, 35% yield to 3-ethynyldiphenylacetylene) as dark yellow solid. **^{1}H NMR** (700 MHz, $CDCl_3$): δ 11.67 (s, 2H), 10.04 (s, 4H), 9.35 (s, 4H), 9.27 (s, 4H), 9.21 (s, 4H), 7.42-7.26 (m, 24H), 2.37 (s, 24H), 2.32 (s, 24H); **^{13}C NMR** (175 MHz, $CDCl_3$): δ 142.8, 142.5, 141.2, 140.9, 137.2, 136.8, 131.8, 131.8, 131.8, 131.7, 128.9, 128.0, 128.0, 128.0, 127.9, 125.3, 125.2, 125.1, 125.0, 124.3, 124.2, 124.2, 124.2, 124.1, 122.0, 121.9, 121.6, 21.7, 21.6; **MS** (MALDI-TOF, positive) calcd. for $C_{136}H_{90}$: *m/z* 1723.7 ($[M+H]^+$), found: *m/z* 1723.2 ($[M+H]^+$).

9.2. ^{1}H and ^{13}C NMR spectra

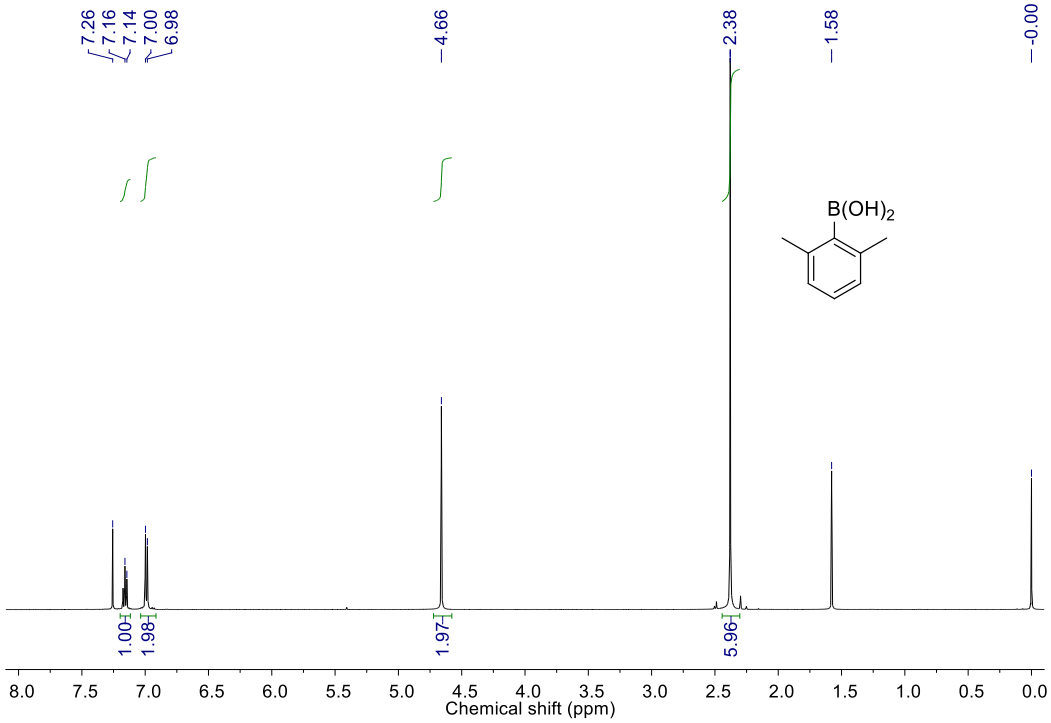

Figure S15. ^{1}H NMR spectrum of the compound **PF-B(OH)$_2$** (500 MHz, $CDCl_3$).

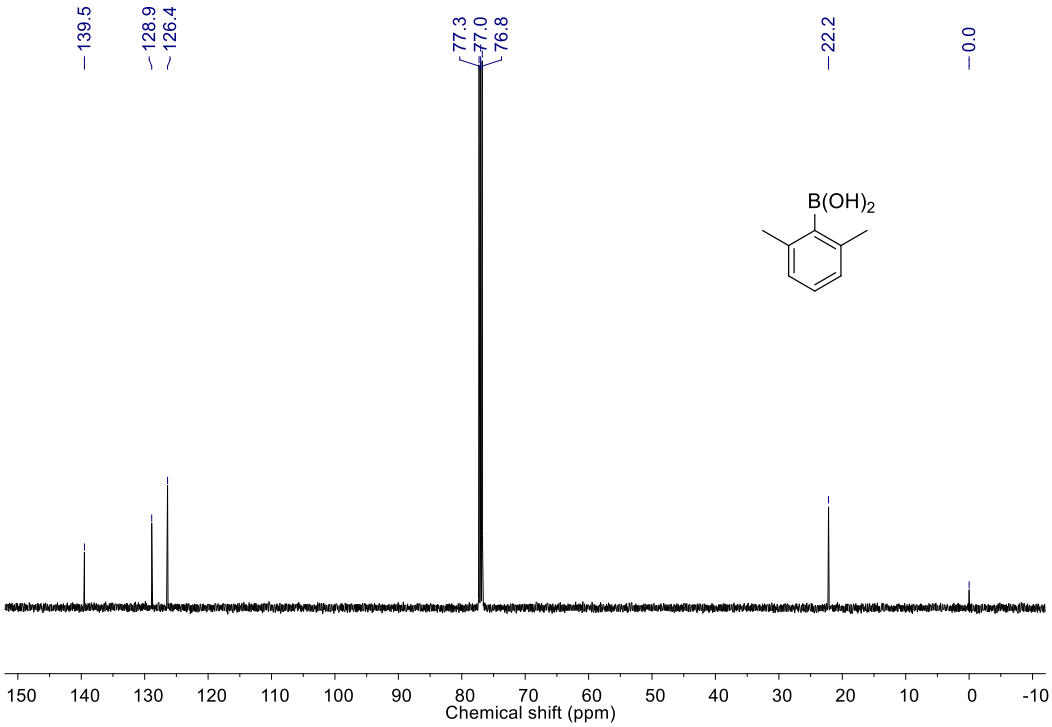

Figure S16. ^{13}C NMR spectrum of the compound **PF-B(OH)$_2$** (125 MHz, $CDCl_3$).

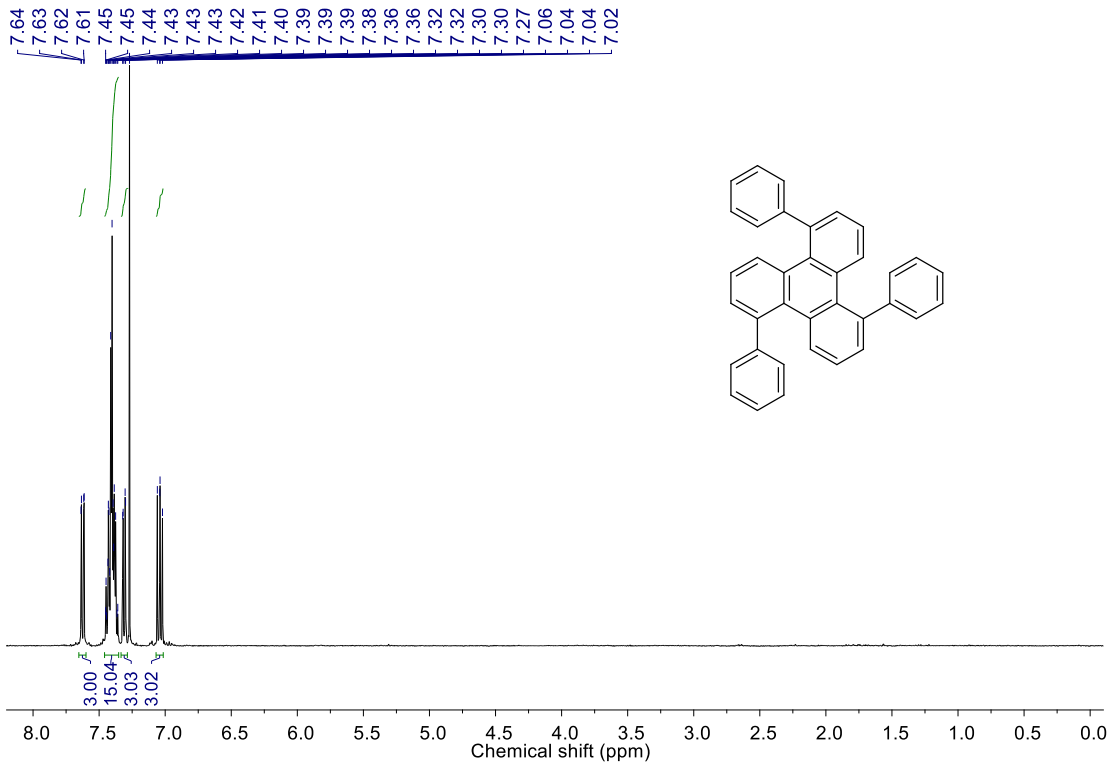

Figure S17. ^{1}H NMR spectrum of the compound **TP-Ph3** (400 MHz, $CDCl_3$).

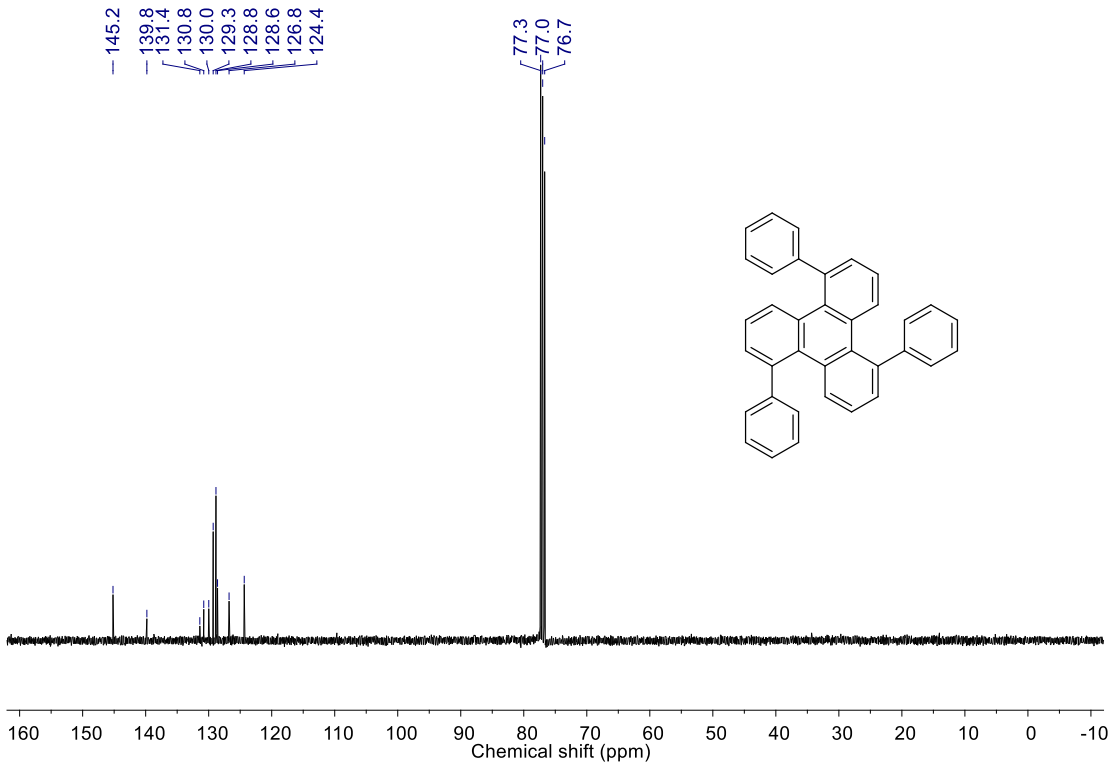

Figure S18. ^{13}C NMR spectrum of the compound **TP-Ph3** (100 MHz, $CDCl_3$).

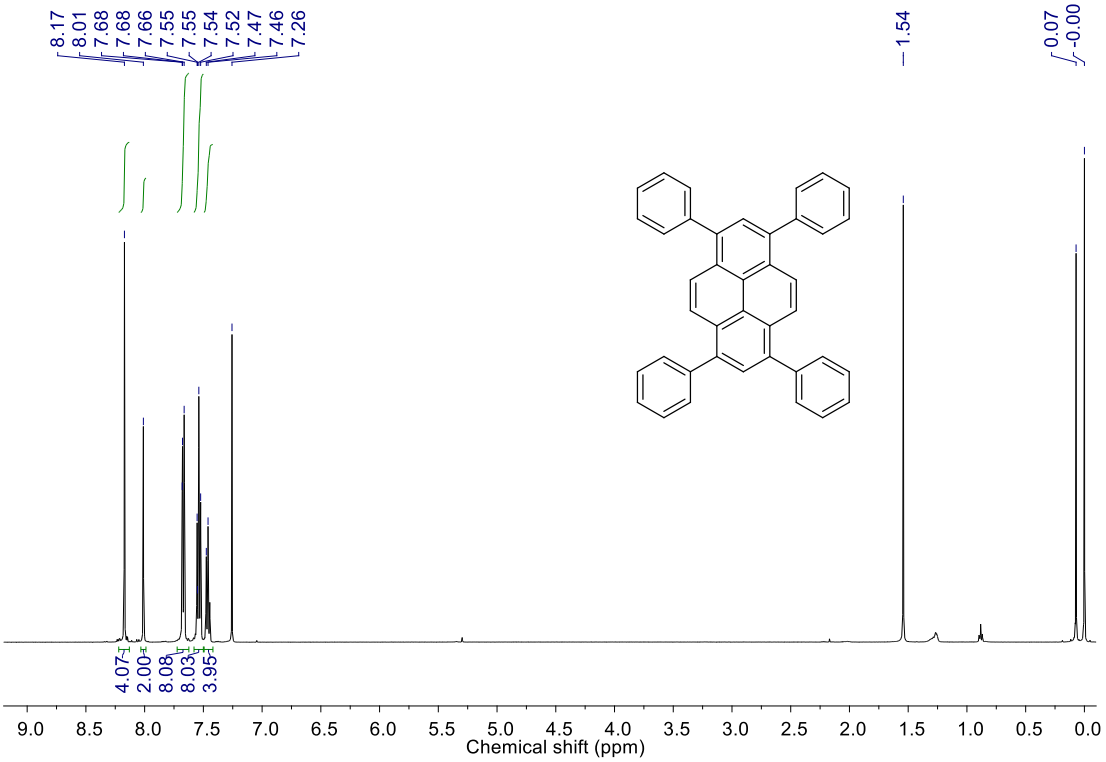

Figure S19. ^{1}H NMR spectrum of the compound **Py-Ph4** (500 MHz, $CDCl_3$).

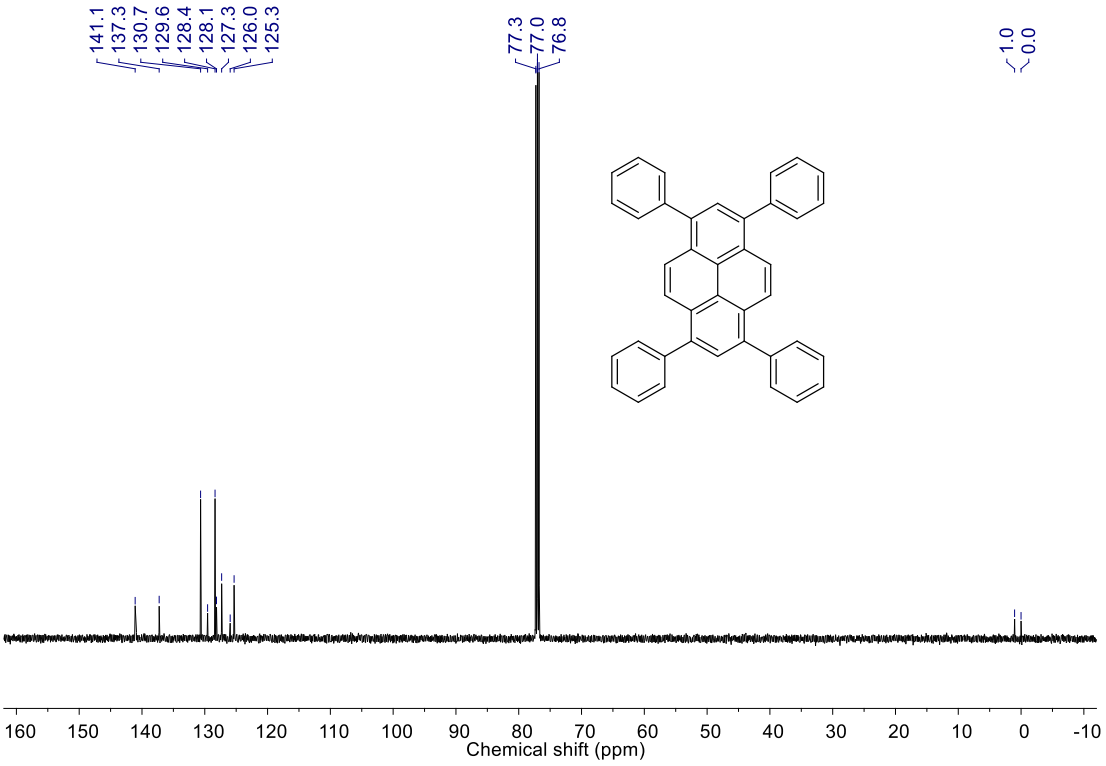

Figure S20. ^{13}C NMR spectrum of the compound **Py-Ph4** (125 MHz, $CDCl_3$).

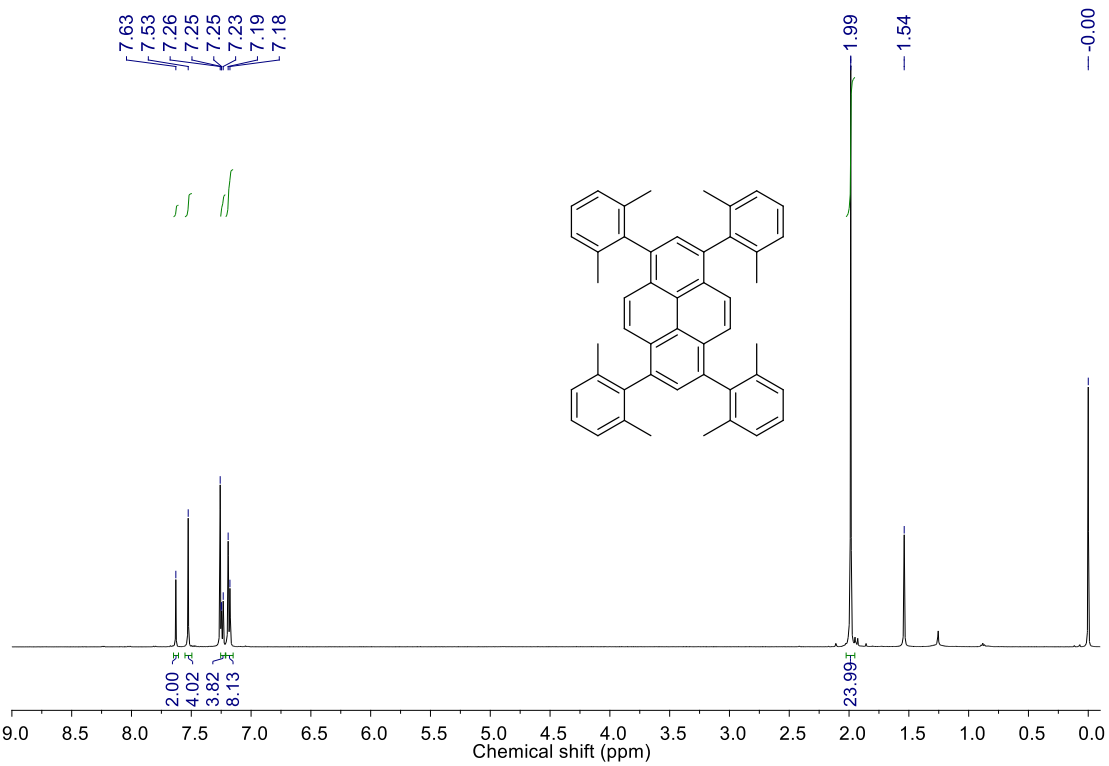

Figure S21. ^{1}H NMR spectrum of the compound **Py-PF4** (500 MHz, $CDCl_3$).

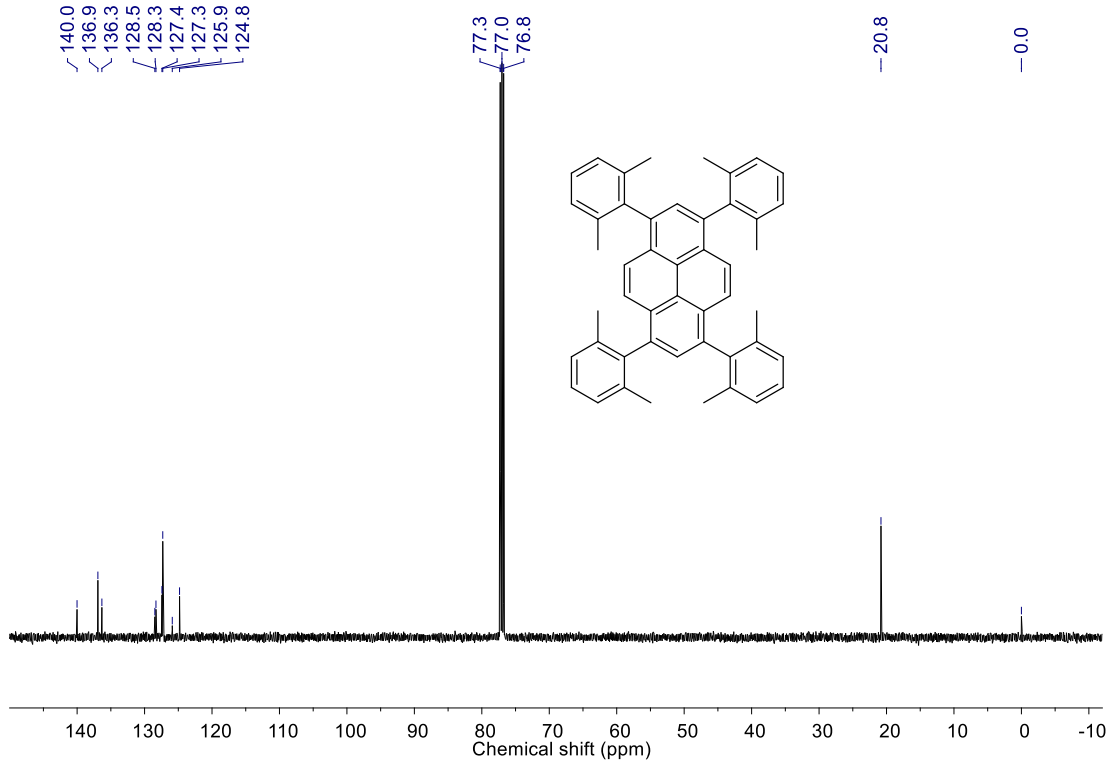

Figure S22. ^{13}C NMR spectrum of the compound **Py-PF4** (125 MHz, $CDCl_3$).

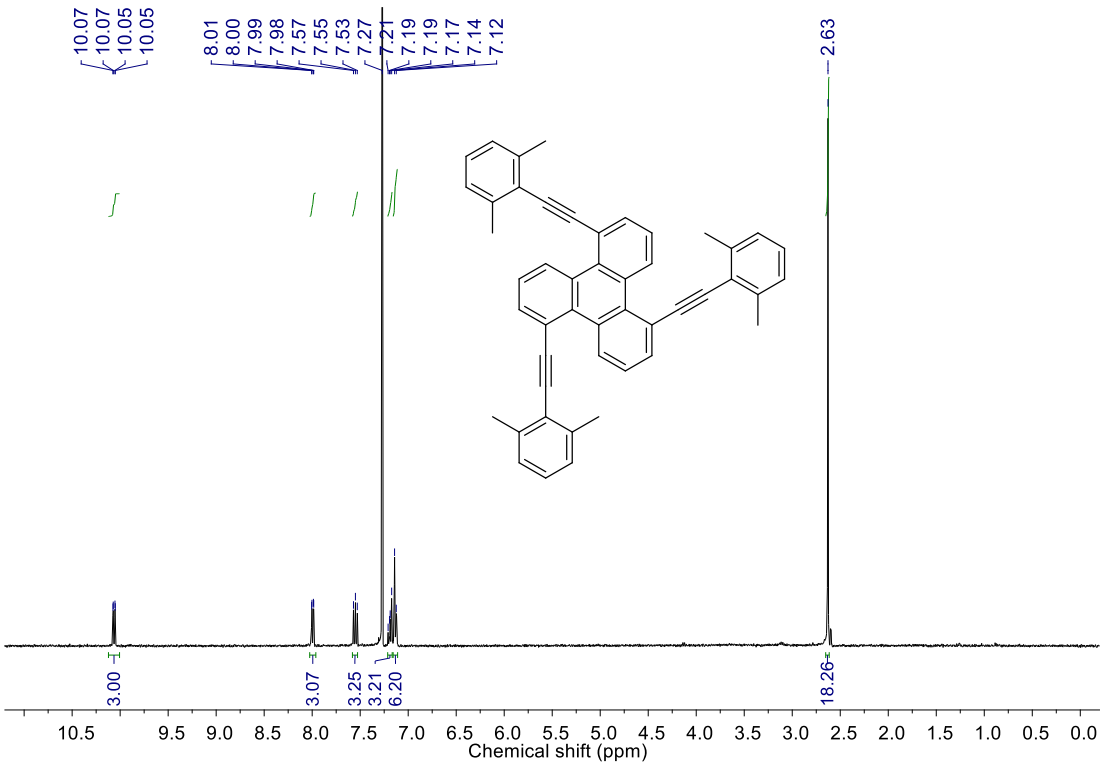

Figure S23. ^{1}H NMR spectrum of the compound **S1** (400 MHz, $CDCl_3$).

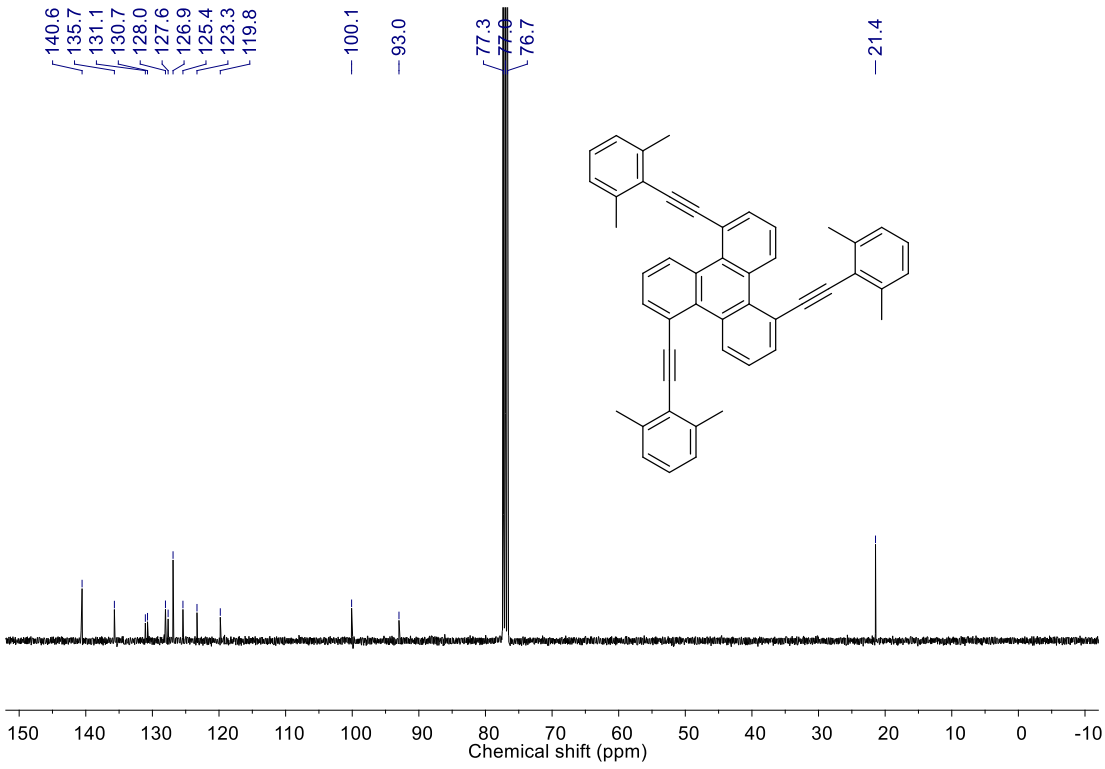

Figure S24. ^{13}C NMR spectrum of the compound **S1** (100 MHz, $CDCl_3$).

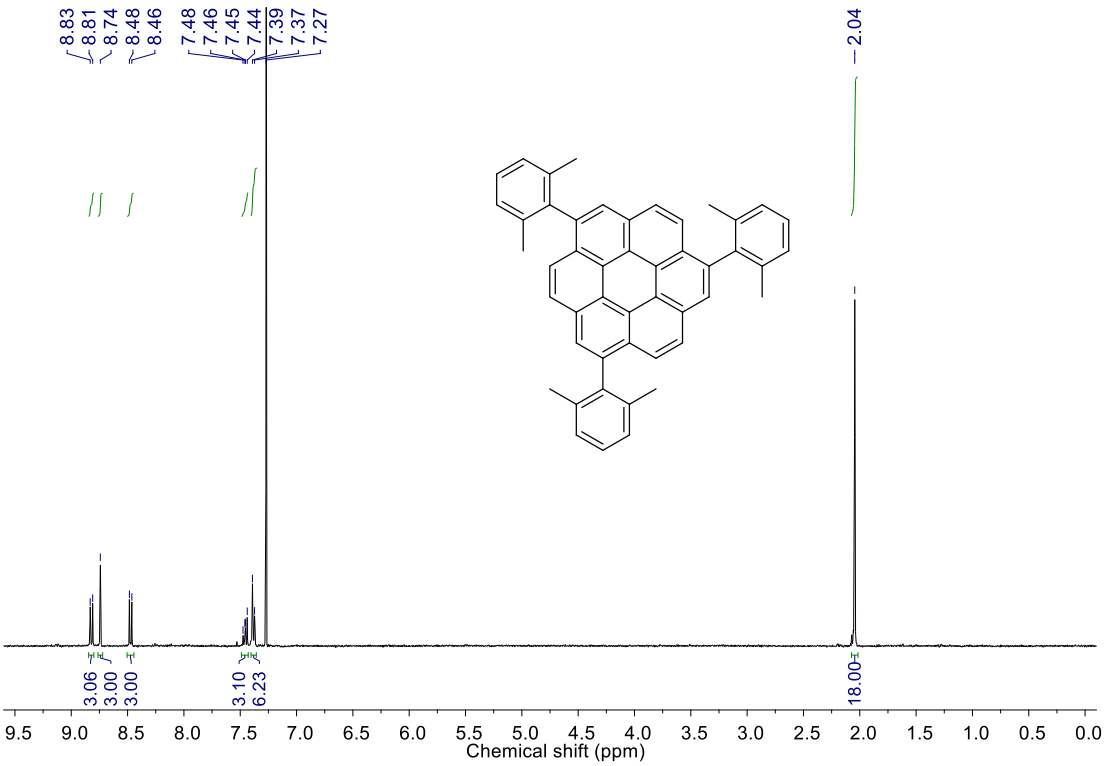

Figure S25. ^{1}H NMR spectrum of the compound **Cor-PF3** (400 MHz, $CDCl_3$).

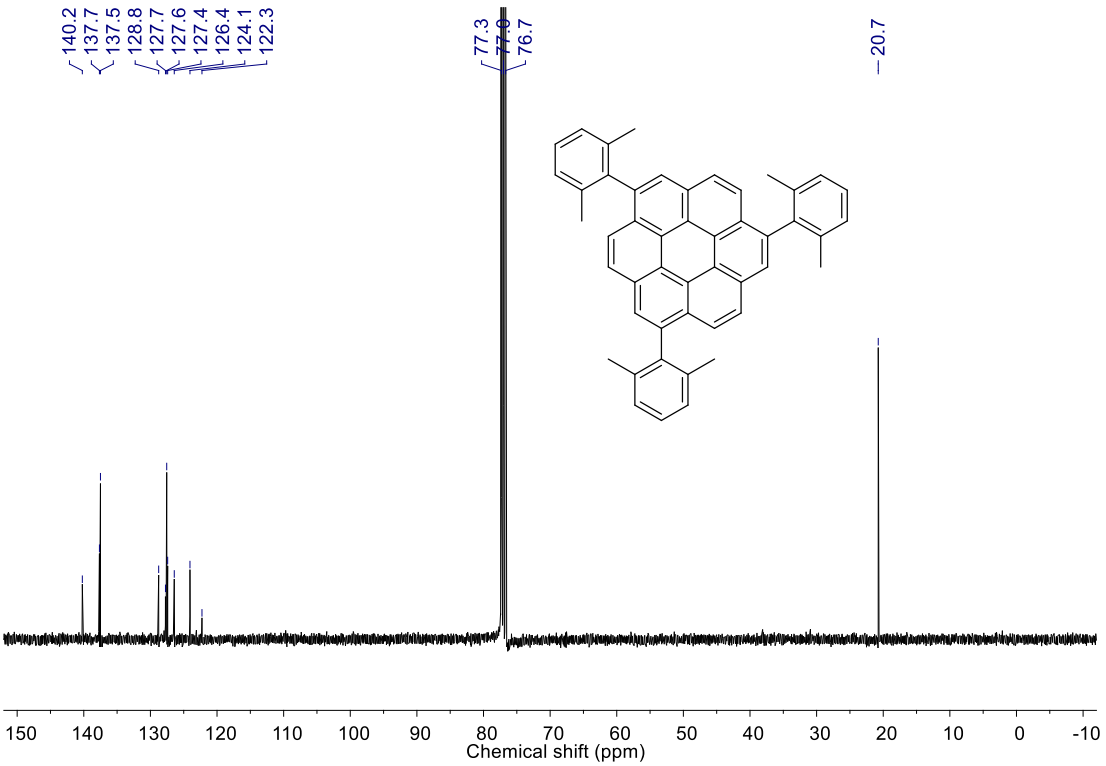

Figure S26. ^{13}C NMR spectrum of the compound **Cor-PF3** (100 MHz, $CDCl_3$).

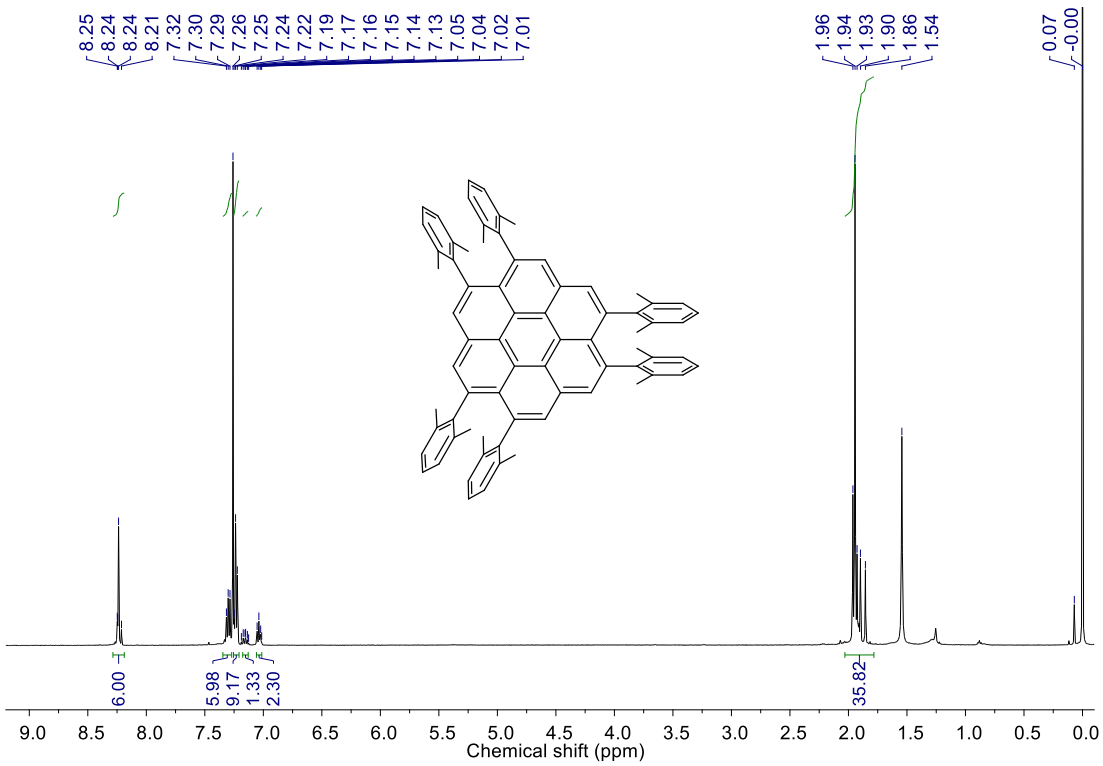

Figure S27. ^{1}H NMR spectrum of the compound **Cor-PF6** (500 MHz, $CDCl_3$).

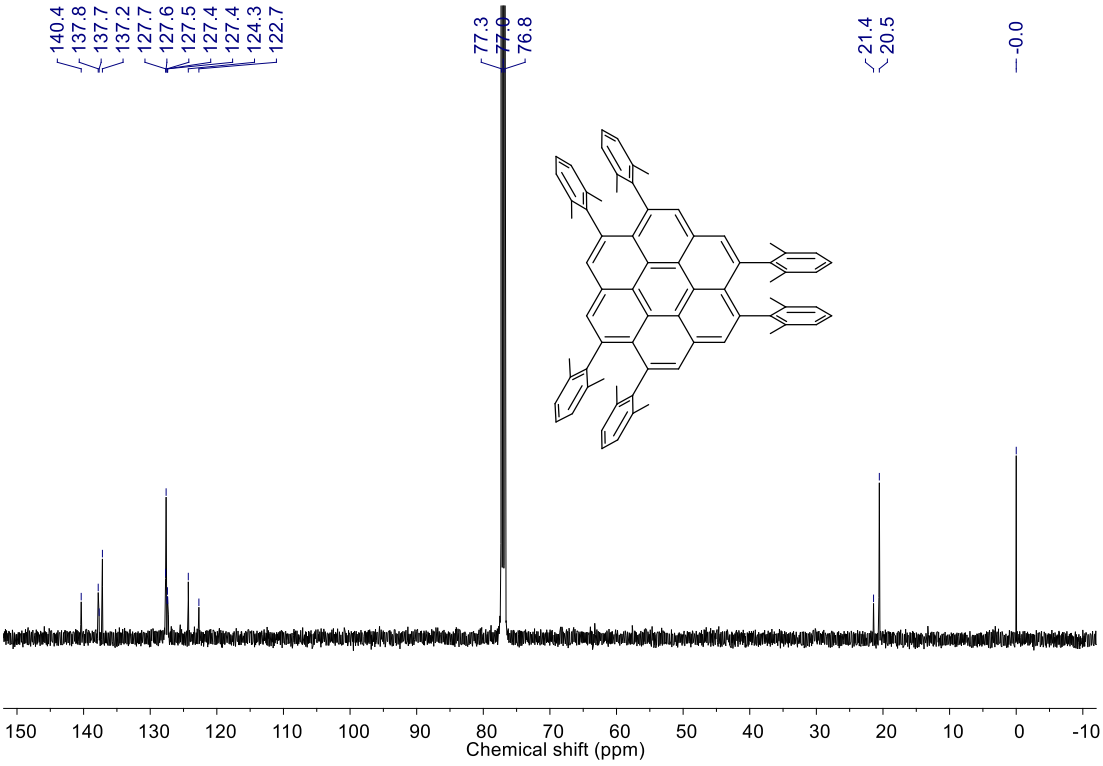

Figure S28. ^{13}C NMR spectrum of the compound **Cor-PF6** (125 MHz, $CDCl_3$).

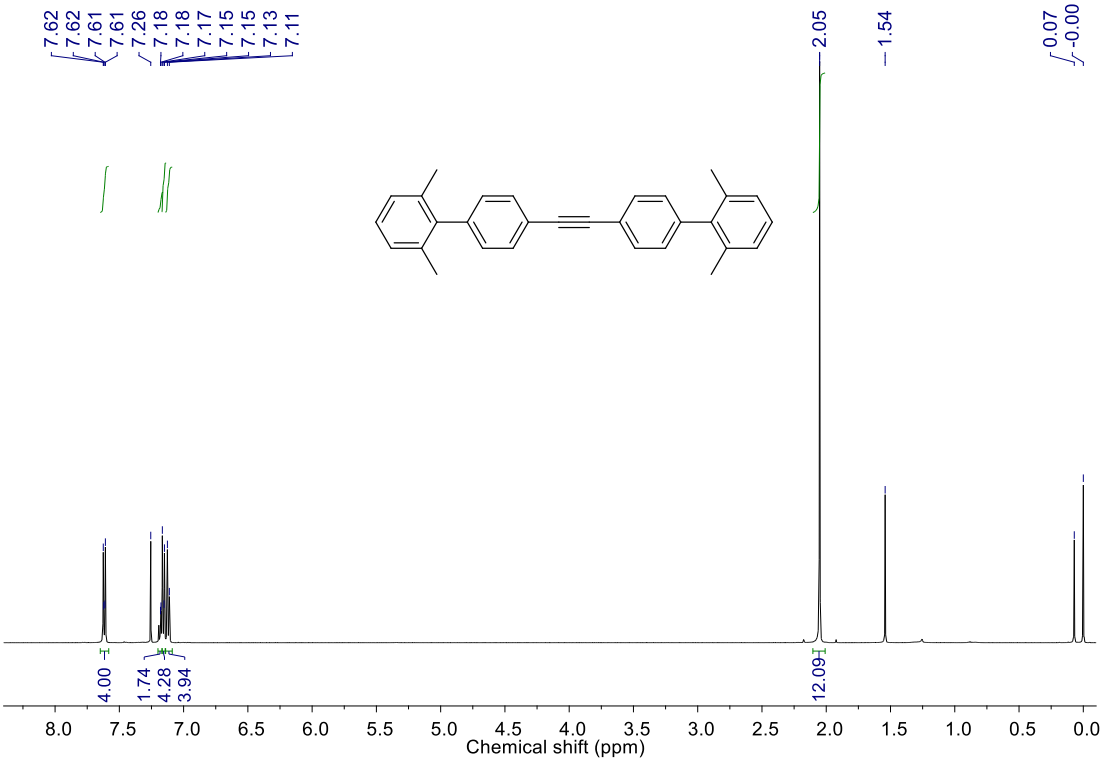

Figure S29. ^{1}H NMR spectrum of the compound **S3** (500 MHz, $CDCl_3$).

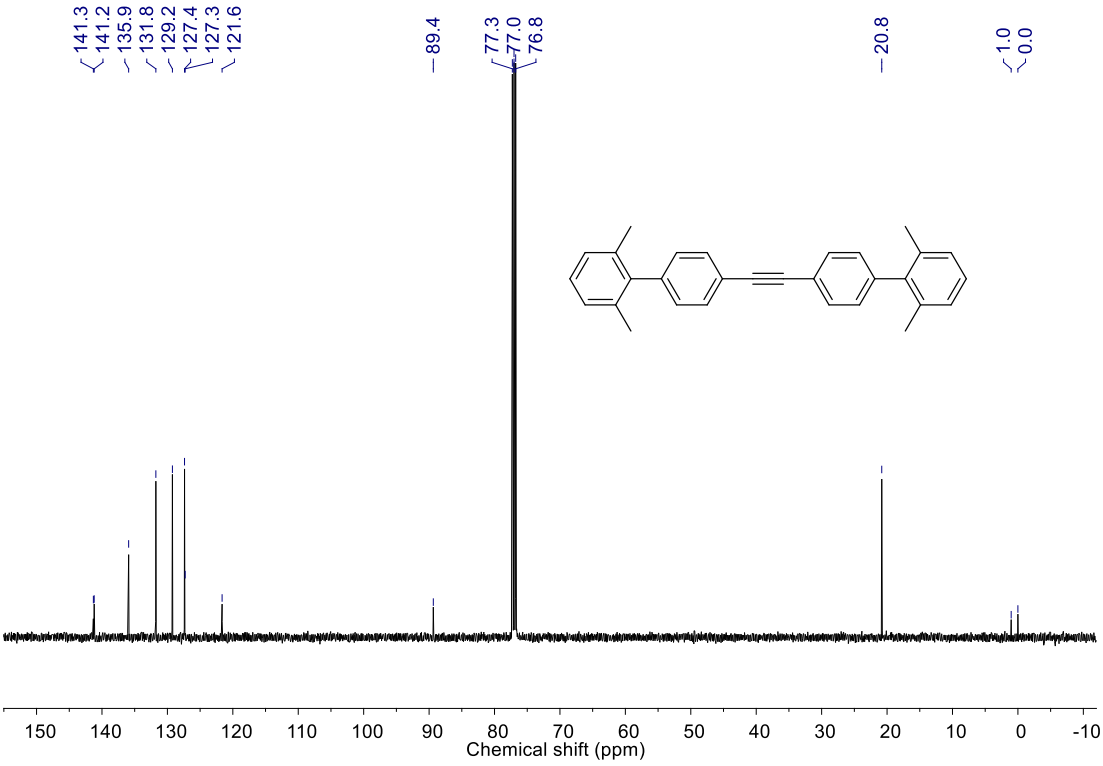

Figure S30. ^{13}C NMR spectrum of the compound **S3** (125 MHz, $CDCl_3$).

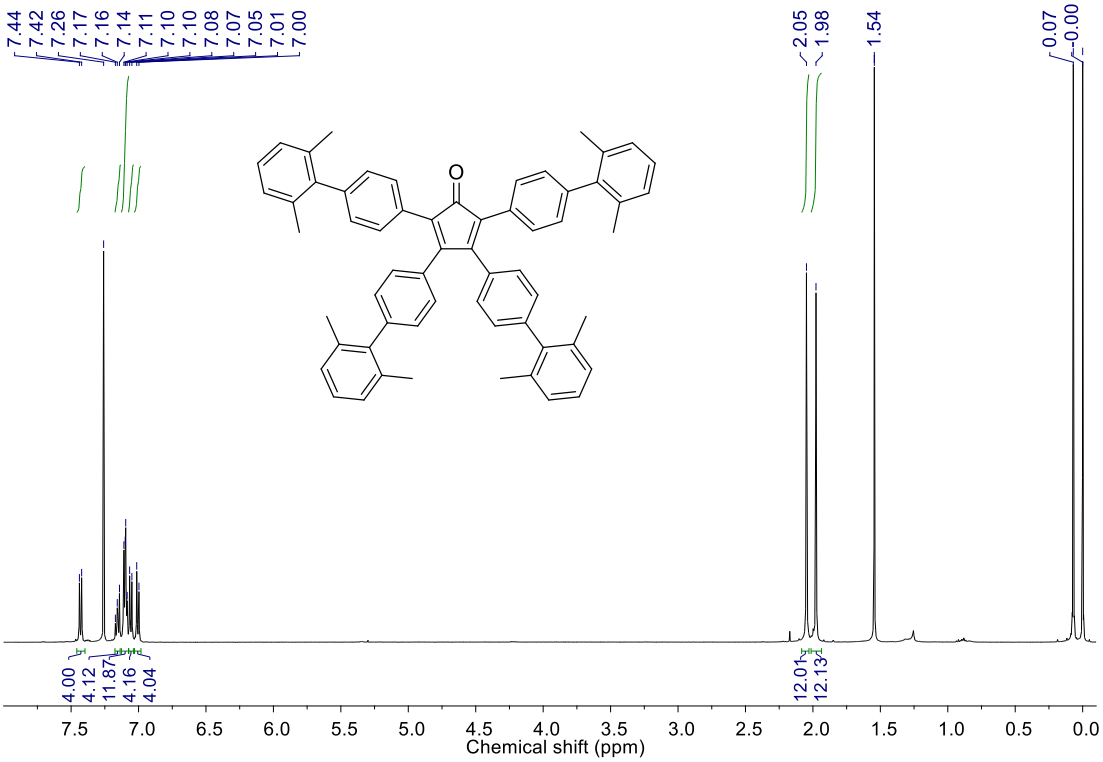

Figure S31. ^{1}H NMR spectrum of the compound **S4** (500 MHz, $CDCl_3$).

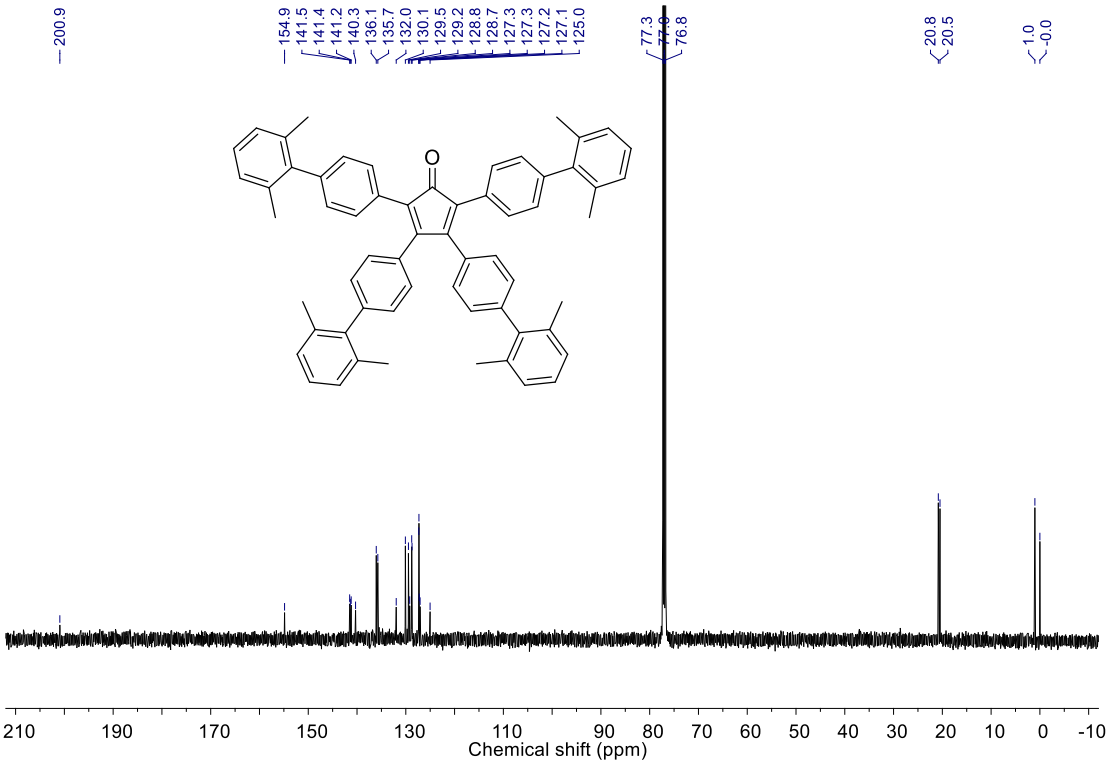

Figure S32. ^{13}C NMR spectrum of the compound **S4** (125 MHz, $CDCl_3$).

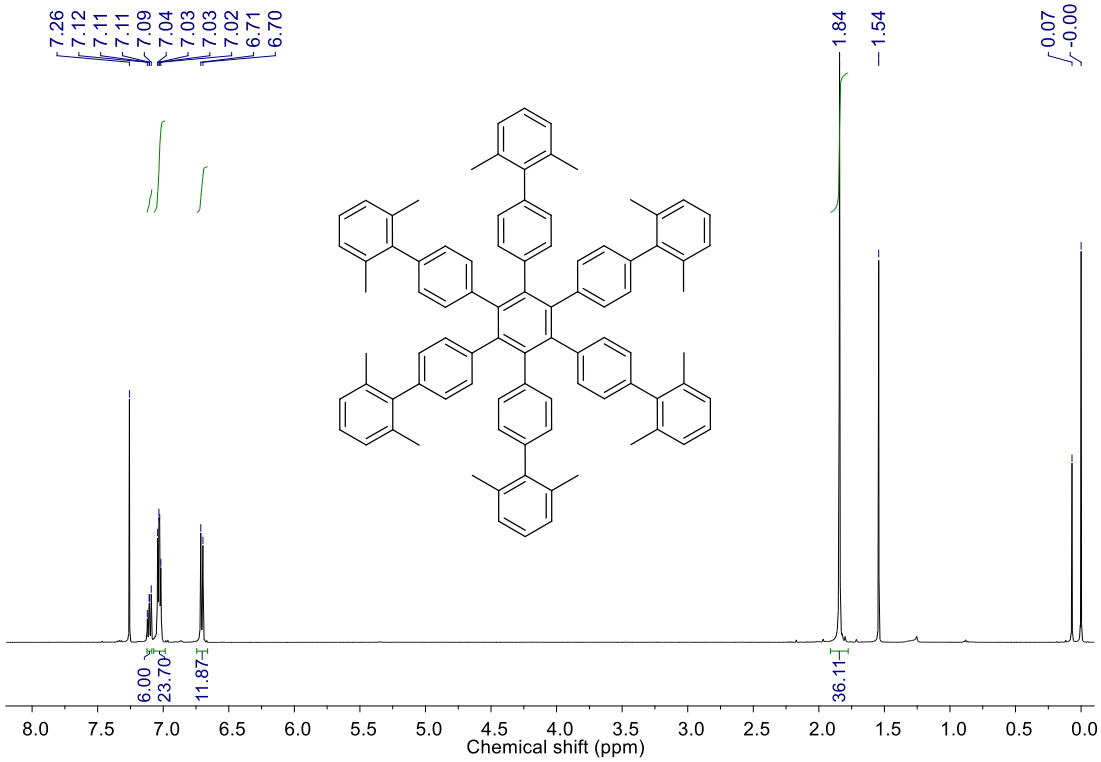

Figure S33. ^{1}H NMR spectrum of the compound **HPB-PF6** (500 MHz, $CDCl_3$).

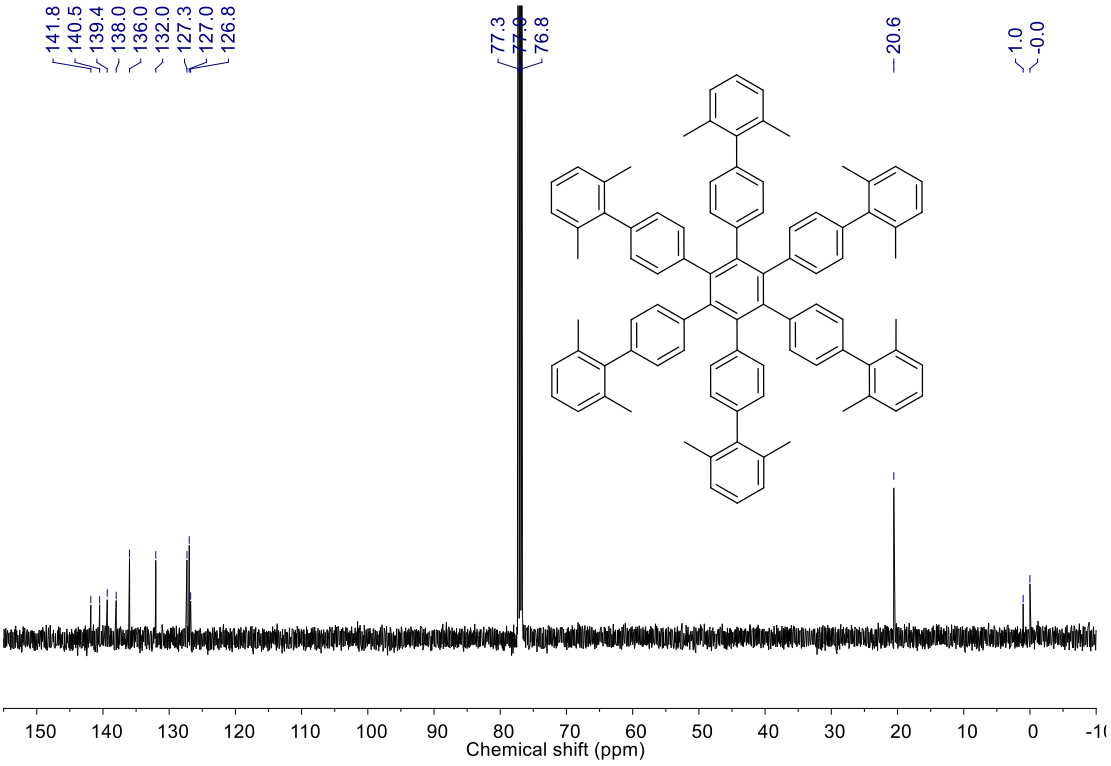

Figure S34. ^{13}C NMR spectrum of the compound **HPB-PF6** (125 MHz, $CDCl_3$).

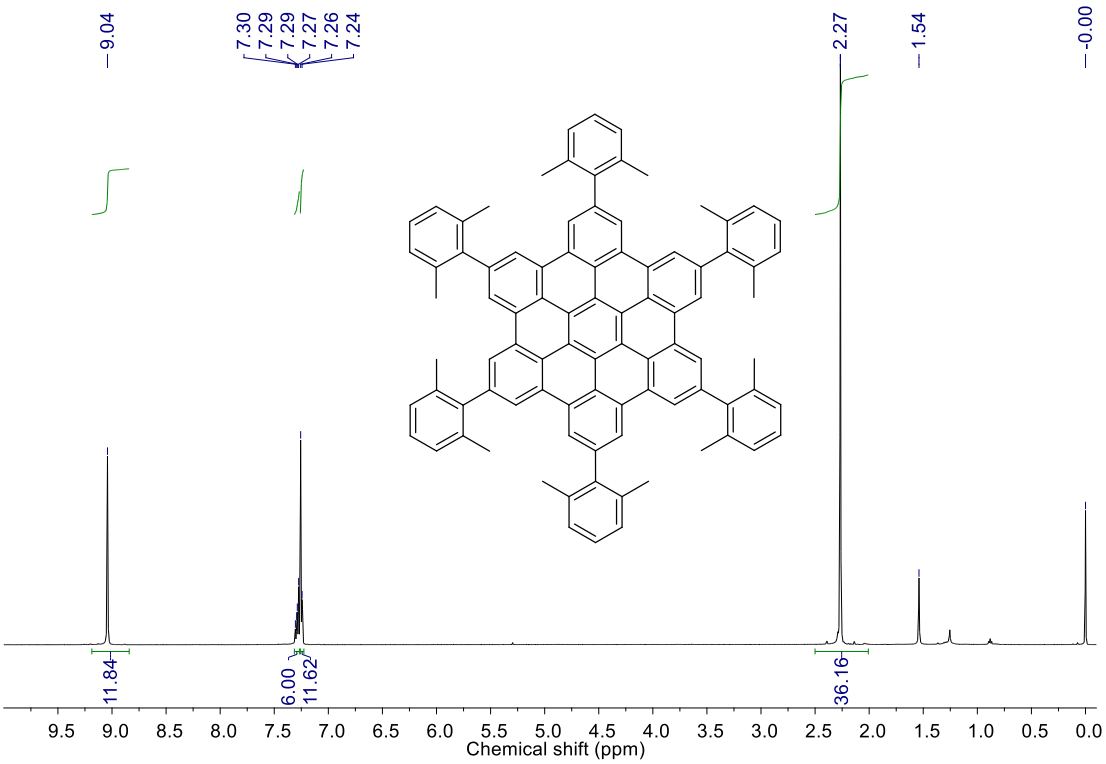

Figure S35. ^{1}H NMR spectrum of the compound **HBC-PF6** (500 MHz, $CDCl_3$).

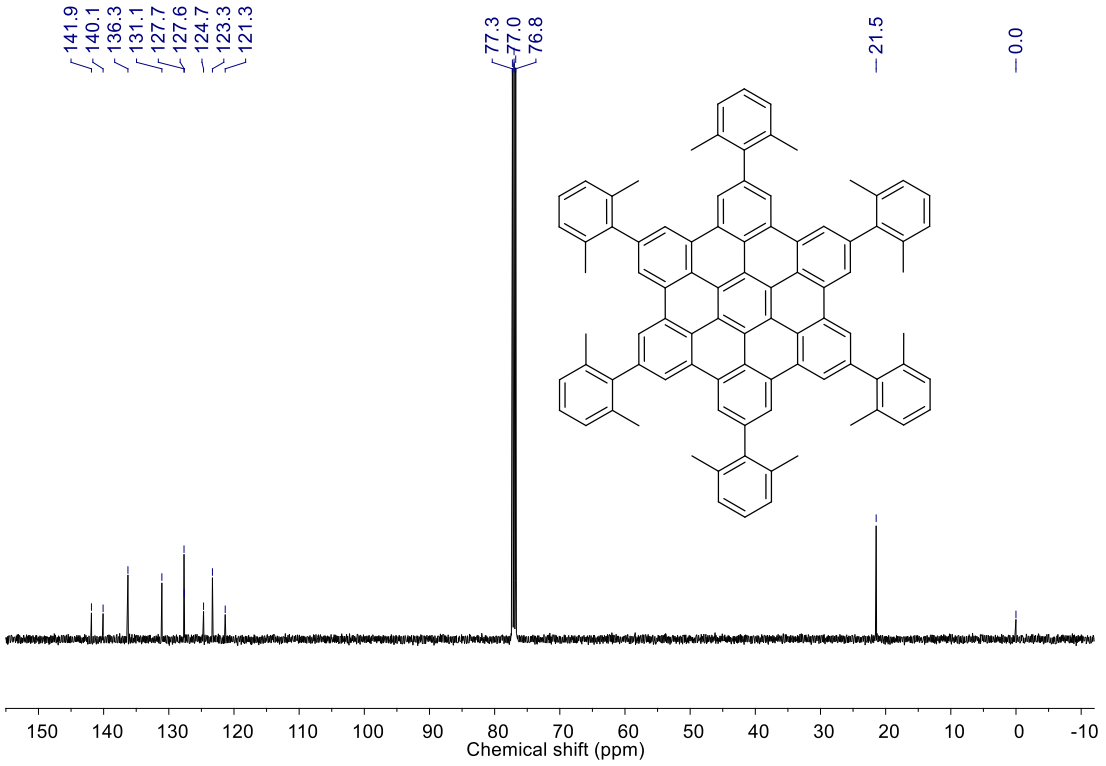

Figure S36. ^{13}C NMR spectrum of the compound **HBC-PF6** (125 MHz, $CDCl_3$).

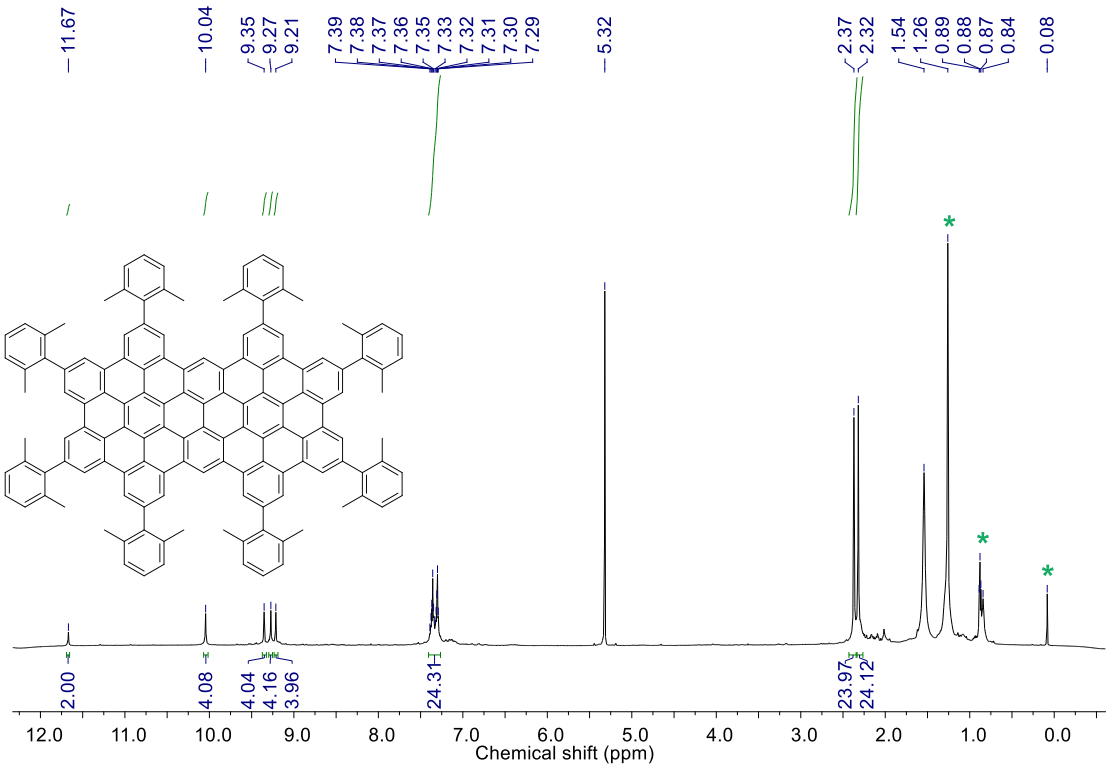

Figure S37. ^{1}H NMR spectrum of the compound **sNAP-PF8** (500 MHz, $CDCl_3$).

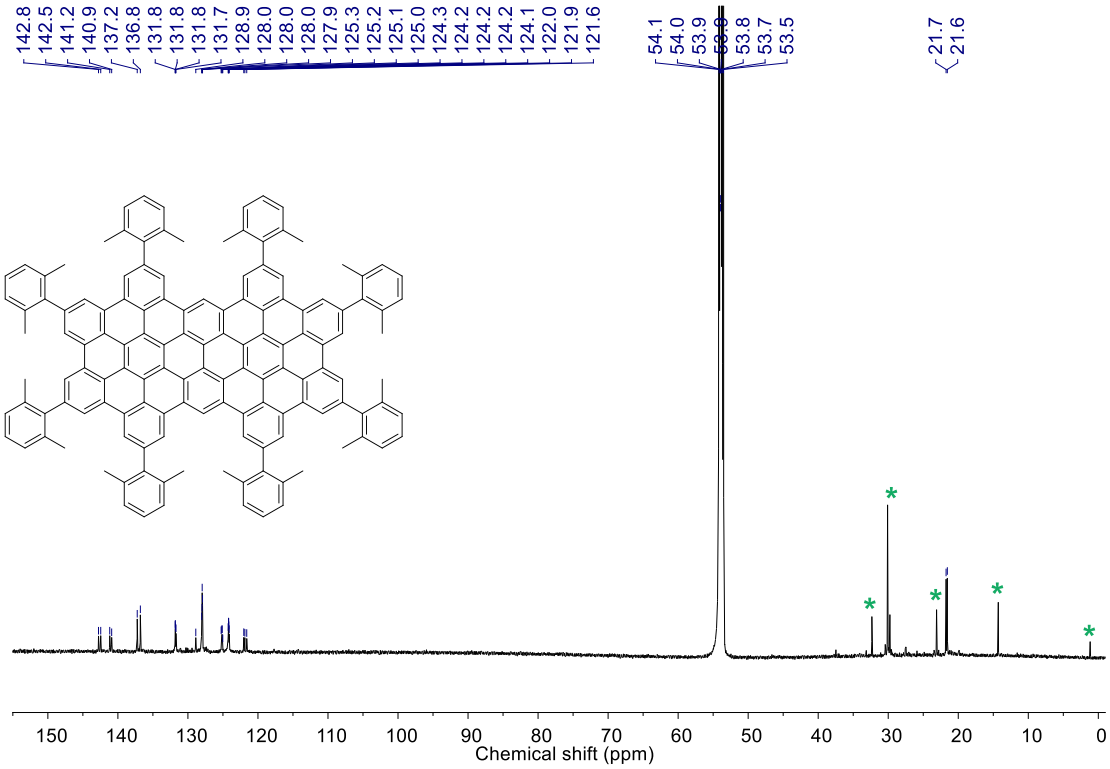

Figure S38. ^{13}C NMR spectrum of the compound **sNAP-PF8** (175 MHz, $CDCl_3$). (* peaks arise due to the hexane and grease included in the sample.)

9.3. MALDI-TOF mass spectra

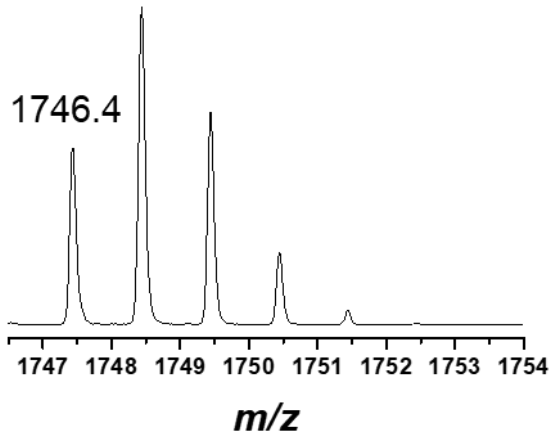

Figure S39. Isotropic distribution of **PP-PF8** obtained by MALDI-TOF MS.

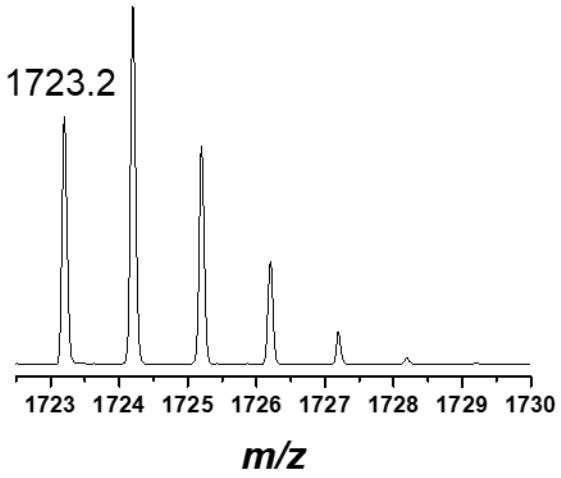

Figure S40. Isotropic distribution of **sNAP-PF8** obtained by MALDI-TOF MS.

10. Reference

1. J. M. Hughes, Y. Hernandez, D. Aherne, L. Doessel, K. Mullen, B. Moreton, T. W. White, C. Partridge, G. Costantini, A. Shmeliov, M. Shannon, V. Nicolosi and J. N. Coleman, *J. Am. Chem. Soc.,* 2012, **134**, 12168-12179.
2. M. P. Johansson and J. Olsen, *J. Chem. Theory Comput.,* 2008, **4**, 1460-1471.
3. A. M. Brouwer, *Pure Appl. Chem.,* 2011, **83**, 2213-2228.
4. H. J. Yvon, *HORIBA Jobin Yvon Inc, Stanmore, Middlesex, UK*, 2012.
5. T T. H. El-Assaad, M. Auer, R. Castaneda, K. M. Hallal, F. M. Jradi, L. Mosca, R. S. Khnayzer, D. Patra, T. V. Timofeeva, J. L. Bredas, E. J. W. List-Kratochvil, B. Wex and B. R. Kaafarani, *J. Mater. Chem. C,* 2016, **4**, 3041-3058.
6. D. Karpovich and G. Blanchard, *J. Phys. Chem.*, 1995, **99**, 3951-3958.
7. T. Kobayashi and S. Nagakura, *Mol. Phys.*, 1972, **23**, 1211-1221.
8. Y. Xia, M. Zhang, S. Ren, J. Song, J. Ye, M. G. Humphrey, C. Zheng, K. Wang and X. Zhang, *Org. Lett.,* 2020, **22**, 7942-7946.
9. E. Fresta, K. Baumgartner, J. Cabanillas-Gonzalez, M. Mastalerz and R. D. Costa, *Nanoscale Horiz.,* 2020, **5**, 473-480.
10. E. Fresta, J. Dosso, J. Cabanillas-Gonzalez, D. Bonifazi and R. D. Costa, *Adv. Funct. Mater.,* 2020, **30**, 1906830.
11. V. V. Jarikov, *J. Appl. Phys.,* 2006, **100**, 014901.
12. K. Usui, K. Tanoue, K. Yamamoto, T. Shimizu and H. Suemune, *Org. Lett.,* 2014, **16**, 4662-4665.
13. H. Kang, A. Facchetti, H. Jiang, E. Cariati, S. Righetto, R. Ugo, C. Zuccaccia, A. Macchioni, C. L. Stern, Z. F. Liu, S. T. Ho, E. C. Brown, M. A. Ratner and T. J. Marks, *J. Am. Chem. Soc.,* 2007, **129**, 3267-3286.
14. Y. Li, Y. X. Wang, X. K. Ren and L. Chen, *Mater. Chem. Front.,* 2017, **1**, 2599-2605.
15. D. D. Zhou, Y. Gao, B. X. Liu, Q. T. Tan and B. Xu, *Org. Lett.,* 2017, **19**, 4628-4631.
16. M. J. Mio, L. C. Kopel, J. B. Braun, T. L. Gadzikwa, K. L. Hull, R. G. Brisbois, C. J. Markworth and P. A. Grieco, *Org. Lett.,* 2002, **4**, 3199-3202.
17. G. Vives and G. Rapenne, *Tetrahedron,* 2008, **64**, 11462-11468.
18. X. Yan, X. Cui, B. S. Li and L. S. Li, *Nano Lett.,* 2010, **10**, 1869-1873.